学 位 論 文

Copper Fine Particles for Electroconductive Materials

（電気導電性材料用銅微粒子）

Yingqiong Yong

Division of Materials Science and Engineering

Graduate School of Engineering, Hokkaido University

Abstract

Conductive inks have received increasing attention over past few decades owing to their applications for printed devices such as light-emitting diodes (LEDs), circuit, flexible displays, radio frequency identification (RFID) tags, and photovoltaics. Because of the lowest resistivity and anti-oxidation properties in air, silver inks are the currently favored conductive inks for printed electronics. However, the high cost and low electro-migration resistance of silver inks which can cause circuit failure under high humidity, limit their applications on a large scale.

Copper, owing to its low cost, low resistivity (1.7×10^{-8} Ω m, similar to that of silver) and high electro-migration resistance, has become the promising material for conductive inks. However, copper particles suffer from the oxidation. This problem can be solved by stabilizing copper particles by surfactants. The stabilizers which act as barriers hinder the percolation paths of electrons, resulting in low conductivity (high resistivity) of the printed patterns. A conventional method to overcome the above obstacle is high temperature sintering in an oven (>250℃). Nevertheless, for applications of low-cost and flexible electronic devices on heat-sensitive substrates, a low sintering temperature is essential. To decrease sintering temperature, several methods, such as laser process, decreasing particle size, photonic sintering, and using copper-based metal-organic decomposition (MOD), have been reported.

In this thesis, new strategies to obtain highly conductive copper layers by lower temperature (≤200 ℃) sintering were put forward. This thesis contains 5 chapters.

First chapter is Introduction. Recent progress of low temperature sintering for electro conductive layers is discussed. In addition, the strategies and methods of the research in this thesis are outlined.

In the second chapter, alkylamine-stabilized copper fine particles and their inks were prepared. One common way to lower the sintering temperature is decreasing particle size (<100 nm). However, this method is complicated and nanoparticles are chemically unstable during storage. In this chapter, a two-step process, in which a facile thermal oxidation process was introduced to increase the contacts between particles, was studied for effective sintering of copper fine particles (>100 nm). In the first step, copper fine particles (280 nm) were synthesized by a one-pot reaction utilizing D-isoascorbic acid as a mild reductant. For sintering processes, an oxidative preheating of the film was used for the formation of tight connections between particles. Then a following reductive sintering using a 3% hydrogen in nitrogen gas at 200 ℃ and 250 ℃ enabled the achieving of high conductivities of copper films. The results showed that the thermal-preheating step in air generated convex surfaces, nanorods or nanoparticles among particles successfully. This was owed to the inside-out diffusion of copper ions from copper particles and the diffusion of oxygen

ion in the opposite direction. The generated convex surfaces, nanorods or nanoparticles increased the contacts between particles and thus facilitated the sintering of particles in the following reductive sintering process. As a result, resistivities of 12.2×10^{-8} and 7.8×10^{-8} Ω m of copper films were achieved at 200 ℃ and 250 ℃, respectively.

In the third chapter, low temperature deposition of metallic copper from metal-organic compound systems is discussed. To achieve low resistivity at a lower sintering temperature, copper-based MOD inks with scalability and simplicity were also studied. In this work, the influence of various copper sources (i.e., copper(II) formate tetrahydrate and copper(II) acetate monohydrate) in MOD inks on the resistivity of films was compared. Commercially available copper particles (0.4-2.5 μm) were introduced into the inks to replace the organic components for higher conductivity and reliability of the obtained copper films. The results demonstrated that the resistivity of sintered copper films decreased with the decrease of size of the added commercial particles. The lowest resistivity of 2.6×10^{-7} Ω m was achieved using the inks containing 0.4 μm of added copper particles after sintering at 120 ℃ under nitrogen. In addition, polyvinylpyrrolidone stabilized copper particles (PVP-Cu) with a size range of 127±20 nm instead of the commercial ones were used for preparing MOD inks to demonstrate the general applicability of this method. The resistivity of the obtained copper film using PVP-Cu particles at the sintering temperature of 100 ℃ was 7×10^{-6} Ω m. These results demonstrated that the use of copper particles to replace organic components in MOD inks effectively led to the low resistivity of film after sintering at the temperature as low as 100 ℃ under nitrogen.

In the forth chapter, in order to further decrease the resistivity, polydispersed-submicron copper particles stabilized with decomposable polymer (polypropylene carbonate, PPC) as a main part and a self-reducible copper formate/1-amino-2-propanol (CuF-IPA) complex as an additive were chosen to prepare the MOD inks. The surface modification of copper particles with PPC, using of smaller poly-dispersed particles, and self-reducible copper complex were favorable to obtaining highly conductive copper films at low temperature sintering. The lowest reported resistivity (8.8×10^{-7} Ω m) at the sintering temperature of 100 ℃ under nitrogen was achieved. Such a low sintering temperature with low resistivity was proved to be a result of the dual promotion effects of aminolysis of PPC with IPA and the pyrolysis of CuF-IPA complex. PPC broke down into smaller molecules by aminolysis with IPA, which reduced the steric stabilization for copper particles, and thus enabled particle coalescence and sintering more easily. The generated copper particles from the pyrolysis of CuF-IPA complex directly contributed for creating connections among particles and higher packing density.

The fifth chapter contains conclusions of this thesis. The methods and conductive inks developed in our study are promising for flexible and low-cost printing electronic devices.

Table of Contents

1. General Introduction

1.1 General introduction of materials for printed electronics

Printed electronics have attracted a tremendous attention in the past decade.[1,2] Printed electronics is relevant to the application of the fabrication of electronic devices using printing technologies. Current applications in the market include electro-optic devices,[3] organic photovoltaics,[4] flexible batteries,[5] radio frequency identification (RFID) tags,[6] and some memory devices,[7] etc.

Materials used for printed electronics can be divided into conductors, semiconductors and dielectrics.[8] Conductive ink used for printing electronics includes a conducting material in an aqueous or organic medium and a variety of additives (e.g., binders and surface tension modifiers) which enable optimal performance of this multi-component system.[2] There are three main criterions, including physical properties of the printed device (conductivity, stability, adhesion and optical transparency), compatibility with the printing pattern, and physicochemical properties of the prepared ink, for the choice of a conductive material for the printing electronics.[9]

1.1.1 Conductors

Metal atoms with organic ligands are utilized for the solution deposition of conductors. For the metal particles or flakes, a thermal post-treatment during which the insulating organic ligands are removed is essential to obtain highly conductive films. About

choosing suitable metals, electrical conductivity, cost and ease of handling are taken into account. The ideal metal-based ink should meet the requirements of low cost, low resistivity after deposition process and post-processing and simplicity of preparing, storing, jetting or printing. In terms of resistivity of metals, silver, copper, and gold have the resistivities of 1.59×10^{-8}, 1.72×10^{-8}, and 2.44×10^{-8} Ω m, respectively. Among silver, copper, and gold, silver has the lowest resistivity. In terms of the cost, an ounce of silver spends $17, whereas one ounce of copper cost 20 cents, and one ounce of gold needs $1100.[10] Currently, silver is the most favored metal and has been most reported. Copper has an obstacle of oxidation which needs to be overcome. Gold is too expensive to be applied on a large scale.

Metal oxide based systems have been used for all kinds of display applications primarily owing to the transparency and their excellent oxygen stability, that is allowing for processing in ambient atmosphere without any inert gas or vacuum system.[11] Indium tin oxide (ITO) as the most well-known metal oxides has been used for displays, especially transparent electrodes for all kinds of liquid crystal displays (LCDs). The pre-patterned ITO bottom electrodes used for light-emitting diodes or solar cells are fabricated by sputtering with additional steps (i.e., lithography and etching process).[8]

Conducting polymers (CPs) as the third kind of conductors for printable electronics have excellent solution processability as well as mechanical flexibility and have been used for flexible and transparent electrodes (FTEs). The commercial conducting polymers are PEDOT: PSS (Poly[3,4-EthyleneDiOxyThiophene]

Poly-StyreneSulfonate) or PANI (PolyANIline). But the conductivity of these polymer conductors are several orders of magnitude lower than that of metals.[8] For the complex of PEDOT and PSS, PSS plays the role of a soluble template as well as a counter-ion and for PEDOT.[11]

Carbon-based nanomaterials like carbon nanotubes (CNTs) and graphene belong to another family of materials used for conductive printing materials. Owing to the unique properties, like high intrinsic current mobility, low resistivity and cost, and good mechanical flexibility,[12] CNTs and graphene sheets have great potential for flexible electronics.

1.1.2 Dielectrics

Thin Film Transistor (TFT) devices are three terminal field-effect devices, in which a semiconductor is placed between source and drain electrodes and a dielectric layer is put between a transversal electrode and the semiconductor.[13] For TFT devices, a dielectric layer has a great effect on their stability and performance. A high capacitance C_i is of significance. A high-k material which has a large dielectric constant is preferred to achieve a high capacitance.[8] In addition, the choice of solvent for the dielectric and the interface between the semiconductor and the dielectric are also important.

1.1.3 Semiconductors

Semiconductors can be divided into two classes, which are carbon-based organic materials and inorganic compounds. Generally speaking, inorganic materials have

excellent performance and environmental stability, while carbon-based organic materials have a superior physical properties and processability.[8]

It is well acknowledged that all the semiconductor materials should have a high purity, be environmentally stable and insusceptibility towards oxidation.[14] Oxide semiconductors, especially the amorphous ones, open the door to new areas like paper electronics and are regarded as one kind of promising TFT materials.[15] Amorphous oxides semiconductors (AOS) are high optical transparency and no grain boundaries which is beneficial to mobility.

1.2 Copper-based conductive inks

1.2.1 The problems of copper-based conductive inks

For the next 20 years, the market for printable electronics would exceed $300 billion based on estimation.[16] Hence there is an urgent need for low-cost, environmentally friendly and faster manufacturing techniques and flexible electronics have been developed recent years. For the low-cost flexible electronics, heat-sensitive substrates like paper and polymeric substrate (e.g., polycarbonate (PC), poly(ether ether ketone) (PEEK), polyethylene naphthalate (PEN), polyimide (PI), polyethylene terephthalate (PET), etc.) are required.

Silver inks as a metal-based conductive ink have the advantages of lowest resistivity (1.6×10^{-8} Ω m) of metallic silver compared with other metals and anti-oxidation properties in air. Thus silver inks are the currently favored inks. However, the issues of high cost and low electro-migration resistance of silver which

can lead to circuit failure under high humidity, limit their applications on a large scale.

Copper inks are deemed to be promising candidate for conductive inks because of its low cost, low resistivity of copper (1.7×10^{-8} Ω m, similar to that of silver) and high electromigration resistance. The obstacle of copper inks for practical application is oxidation problem. Copper is easily to be oxidized even in an ambient atmosphere. Stabilizing copper particles by capping layer is a solution for the above problem. In general, these stabilizers which function as barriers can hinder the percolation paths of electrons and thus lead to high resistivity or low conductivity of the printed patterns. In order to achieve high conductivity of printed patterns, high temperature sintering in an oven as a conventional method is frequently used to remove these stabilizers (> 250 ℃). However, to meet the requirement of low-cost and flexible electronic devices which need heat-sensitive substrates, lower sintering temperature is crucial. For example, the glass transition temperature (Tg) of polycarbonate (PC) is 147 ℃; Tg of poly(ethylene naphthalate) is 125 ℃; Tg of polyimide (PI) is 222 ℃.[17]

To decrease the sintering temperature, several methods, such as decreasing particle size to nanoscale, using copper-based metal-organic decomposition (MOD), photonic sintering, have been reported. The following part will introduce these methods in detail.

1.2.2 Possible solutions

Decreasing particle size to nanoscale

According to a classical thermodynamic analysis, Gibbs-Thomson equation, the

melting point of a material is size-dependent. This melting point depression effect is relevant to cohesive energy of the materials.[18] Decreasing particle size can reduce the melting point of particles and thus facilitate particle sintering, leading to a high conductivity of sintered films.

Fig. 1.1 gives the relationship between melting point and particle diameter of gold nanoparticles according to Gibbs-Thomson equation.[19,20] Melting point decreases with the decrease of particle diameter of gold nanoparticles. There is an exponential relationship between the melting point and the particle diameter. When the size becomes around 5 nm, the melting point can be reduced below 200 ℃. The percolation threshold of conductive network can be even lower by the changing the surface morphology of the nanomaterials.[20]

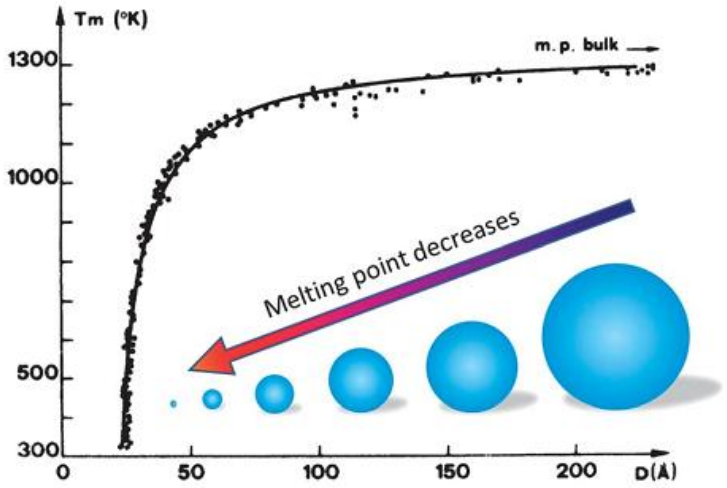

Fig. 1.1 The relationship between the melting point and particle diameter of gold nanoparticles.[20]

Deng and coworkers have described a simple, high throughput, and facile method to prepare copper nanoparticles in an aqueous solution.[21] In this work, copper acetate, hydrazine, and short chain carboxylic acids which have low decomposition

temperature were chosen as copper precursor, reducing agent, and capping agents, respectively. Lactic acid, citric acid, or alanine as the capping agent with high concentration can obtain stable copper nanoparticles which are smaller than 10 nm (particle diameter) and have a narrow size distribution. It was demonstrated that the concentration of the carboxylic acid is important for the preparation of such copper nanoparticles. Thermogravimetric analysis results exhibited that both lactic acid and glycolic acid capped on the surface of the nanoparticles can be removed at a relatively low temperature. For glycolic acid, it can even be removed at about 125 ℃. Copper films obtained from the sintering of lactic acid and glycolic acid capped copper particles can achieve low electrical resistivity at low sintering temperature. After annealing at 150 ℃ for 60 min under nitrogen, the electrical resistivities of the copper film using glycolic acid and lactic acid as the capping agents were 2.6×10^{-7} and 2.1×10^{-7} Ω m, respectively. When the annealing temperature was increased to 200 ℃, the resistivities of the copper film using glycolic acid and lactic acid as the capping agents after annealing for 60 min under nitrogen were 3.5×10^{-7} and 9.1×10^{-8} Ω m, respectively.

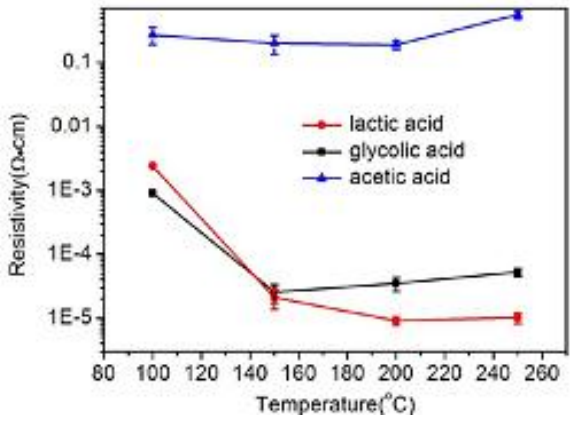

Fig. 1.2 Resistivity of the copper films obtained by sintering different capping agents stabilized copper particles at various temperatures under nitrogen.[21]

Hokita and coworkers have developed a simple, high-concentration synthesis of sub-10-nm Cu NPs in ethylene glycol under ambient air conditions at room temperature.[22] High throughout (90% yield), monodispersed spherical AmIP-Cu NPs with size of 3.5 ± 1.0 nm were synthesized using copper(II) acetate as copper sourceusing, 1-amino-2-propanol (AmIP) as the stabilizer and hydrazine monohydrate as the reducing agent. It was proposed that the single nanosize of AmIP-Cu NPs and their superior stability were due to the formed five-membered ring structure between Cu and AmIP which can enhance the binding force of AmIP onto the Cu surface. After redispersing the AmIP-Cu NPs into alcohol-based solvents, copper inks containing 45 wt% of Cu were prepared. The conductive copper films obtained using Cu nanoink on polyimide film can achieve the electrical resistivity of 3.0×10^{-7} Ω m after thermal annealing at 150 ℃ for 15 min under nitrogen gas (Fig. 1.3). In addition, this work experimentally demonstrated that AmIP can be act as the reducing agent to reduce Cu_2O to metallic copper during the thermal heating process. The adhesion

measurement on PET film was also conducted. The results showed that PET with the UVO treatment can improve the adhesion strength as well as maintain low resistance for Cu nanoinks.

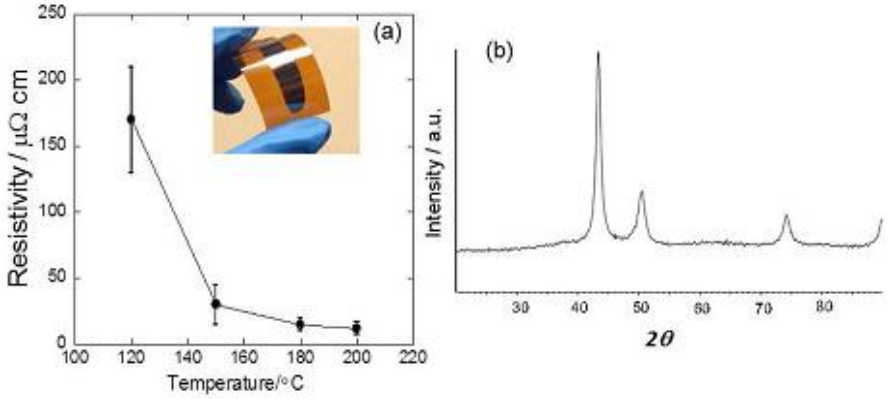

Fig. 1.3 (a) Resistivity of Cu film after the thermal annealing of Cu nanoink which contained 45 wt% Cu in propylene glycol/glycerol solvent [1:1 vol %] on polyimide film for 15 min at various temperatures (120, 150, 180, and 200 ℃). (b) XRD pattern for Cu film after the thermal annealing of Cu nanoink which contained 45 wt% Cu in propylene glycol/glycerol solvent [1:1 vol %] on polyimide film for 15 min at 150 ℃.[22]

Sugiyama and coworkers have synthesized high-concentration (0.3 M copper salt) 2-amino-1-butanol-stabilized Cu nanoparticles (AB-Cu NPs) with a size of 4.4 ± 1.0 nm at room temperature under an ambient condition (Fig. 1.4).[23] The capped AB ligand can form metallacyclic coordination with a five-membered structure with Cu to increase the stability of synthesized Cu particles. In this work, the sintering temperature can be as low as 60 ℃, which is the lowest reported temperature for Cu NPs. Following thermal annealing at 150 ℃ under a nitrogen gas for 30 min, Cu

nanoink consist of AB-Cu NPs (~35 wt% Cu) could produce a Cu film with resistivity of 5.2 $\times 10^{-7}$ Ω m. Furthermore, the adhesion between the Cu film and substrate was also compared. AB-based Cu nanoink had better adhesion to the substrate than 1-amino-2-propanol (AmIP)-based Cu nanoink, which is ascribed to carboxylic compounds generated after the thermal annealing of the Cu nanoinks.

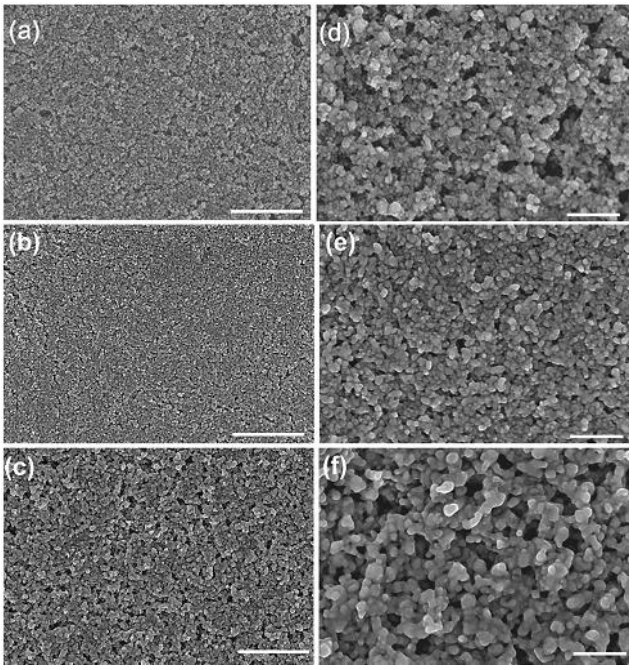

Fig. 1.4 SEM images of sintered Cu films using Cu nanoink on polyimide film for 30 min at a , d 120 °C, b , e 150 °C, and c , f 200 °C. The scale bar of (a, b, c) is 1μm and that of (d, e, f) is 100 nm.[23]

Copper-based metal-organic decomposition (MOD)

Shin and coworkers have prepared alcohol-soluble copper-based MOD ink which is reducible without using a reducing gas.[24] Alcohol-soluble conductive inks are essential for commercial printing processes like reverse offset printing process. In the

prepared ink, copper (II) formate (Cuf) was chosen as a precursor and 2-amino-2-methyl-1-propanol (AMP) was exploited as a ligand to form the complex with copper and to facilitate the decomposition of copper(II) formate. In addition, octylamine (O) as a co-complexing agent and hexanoic acid (H) as a sintering helper were introduced into the system to further obtain well-sintered copper film after heat treatment process. The resistivity of copper-based MOD ink (Cuf-AMP-OH ink) after heating under a nitrogen gas for 30 min at 200, 250, 300, and 350 ℃ were 2.3×10^{-7}, 1.9×10^{-7}, 1.3×10^{-7}, $9.5 \times 10^{-8}\ \Omega$ m, respectively (Fig. 1.5).

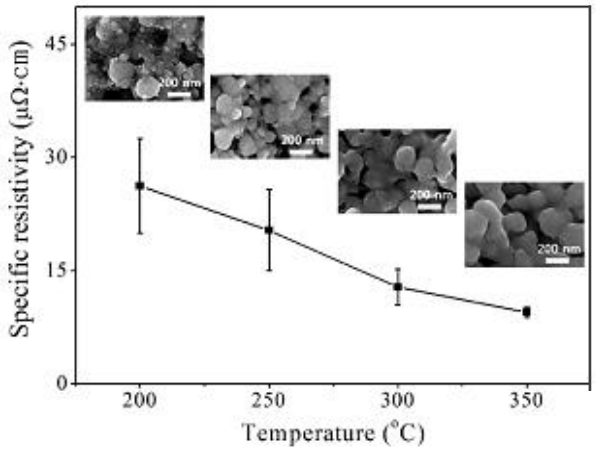

Fig. 1.5 Resistivity of the Cu film obtained using Cuf-AMP-OH ink following heat treatment for 30 min under a nitrogen gas as a function of the heating temperature. The inset images exhibit the morphologies of corresponding sintered Cu film.[24]

Farraj *et al.* presented a self-reduction MOD ink which contained hydrous copper (II) formate (CuF) as copper source and 2-amino-2-methyl-1-propanol (AMP) as the ligand.[25] The decomposition process of CuF-AMP complex and CuF as well as the role of water molecular in the decomposition of complex were investigated using

thermogravimetric and mass spectrometry analyses. The ink underwent pyrolysis of CuF-AMP complex to form metallic copper at low heating temperatures. The produced conductive Cu film could be printed on heat sensitive substrate like PET (polyethylene terephthalate). A low resistivity of 1.1 $\times 10^{-7}$ Ω m was obtained after heat treatment of complex under N_2 at 190 ℃ (Fig. 1.6).

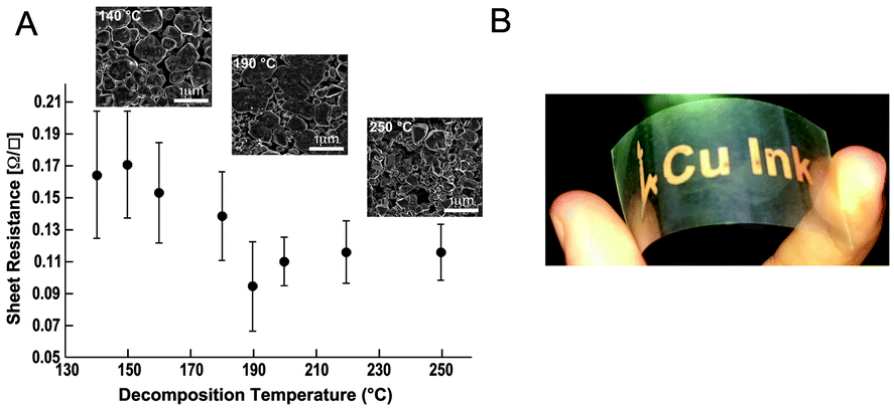

Fig. 1.6 (A) Sheet resistance of obtained conductive Cu films as a function of decomposition temperature. The inset SEM images are corresponding micrographs at various decomposition temperatures. (B) Copper patterns on PET film using the copper complex with ink-jet printing technique.[25]

Kim *et al.* studied the relationship between the resistivity and the copper concentration in copper (II) formate (CuF)-hexylamine complex. The copper concentration controlled impurity content and the porosity of the film, thus finally determining the electrical resistivity of the sintered Cu films. The lowest bulk resistivity, got from the ink which had 12.4 wt% of copper, after heating at 200 ℃ followed by formic acid reduction process at 250 ℃, was 5.2 $\times 10^{-8}$ Ω m.[26]

Yabuki and coworkers have prepared complexes of copper formate and various amines including primary amines and secondary amines. It was demonstrated that the resistivity of sintered copper film and the size of particles are related to the types of amines and the length of the alkylchain (Fig. 1.7). Using the blended amines of dibutylaminethe and octylamine, the lowest resistivity of 5×10^{-8} Ω m could be obtained after annealing at 140 ℃.[27]

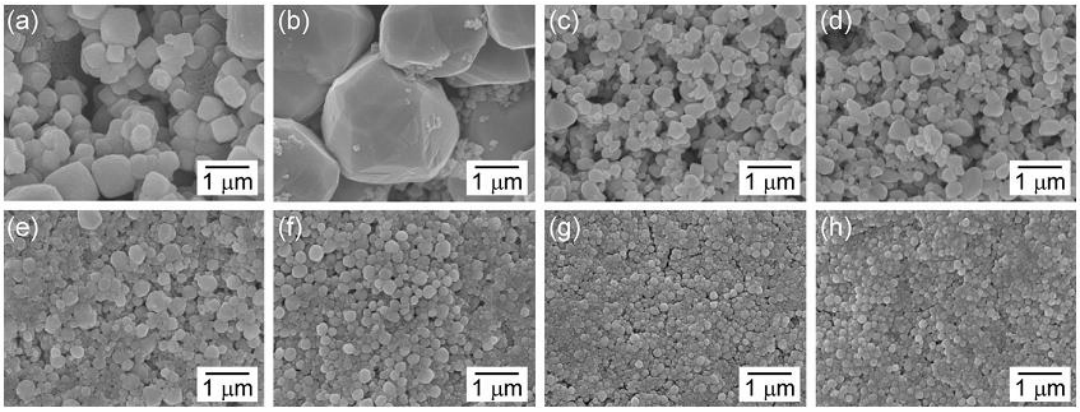

Fig. 1.7 SEM images of obtained Cu films annealed at 140 ℃ for 30 min using copper-amine complexes. The used amines are (a) dipropylamine, (b) dibutylamine, (c) diamylamine, (d) dihexylamine, (e) hexylamine, (f) heptylamine, (g) octylamine, and (h) nonylamine.[27]

Choi *et al.* investigated the nucleation behavior, growth behavior, and sintering process of Cu nanoparticles during thermal heating process of copper (II) formate (CuF)-hexylamine (HA) complex to form metallic copper. It was revealed that the hexylamine (HA) concentration played an important role in the microstructure evolution during the decomposition of complex and electrical resistivity of produced copper film (Fig. 1.8).[28] HA acted as a reducing agent which dissociates the carboxyl

group from the copper precursor as well as a ligand to control the growth of Cu nuclei. Low HA concentration led to the multiple growths of Cu nanoparticles during the heating process, which thus resulting in copper films with porous microstructure and low electrical conductivity. For the CuF-HA complex with a high HA concentration, the sufficient complexation was beneficial to the single-route growth of nanoparticles during the thermal heating process, consequently leading to small Cu nanoparticles with a narrow size distribution and a dense Cu film. The highly conductive Cu film with the lowest resistivity of 4.1×10^{-7} Ω m was obtained at 200 ℃ with a HCOOH atmosphere.

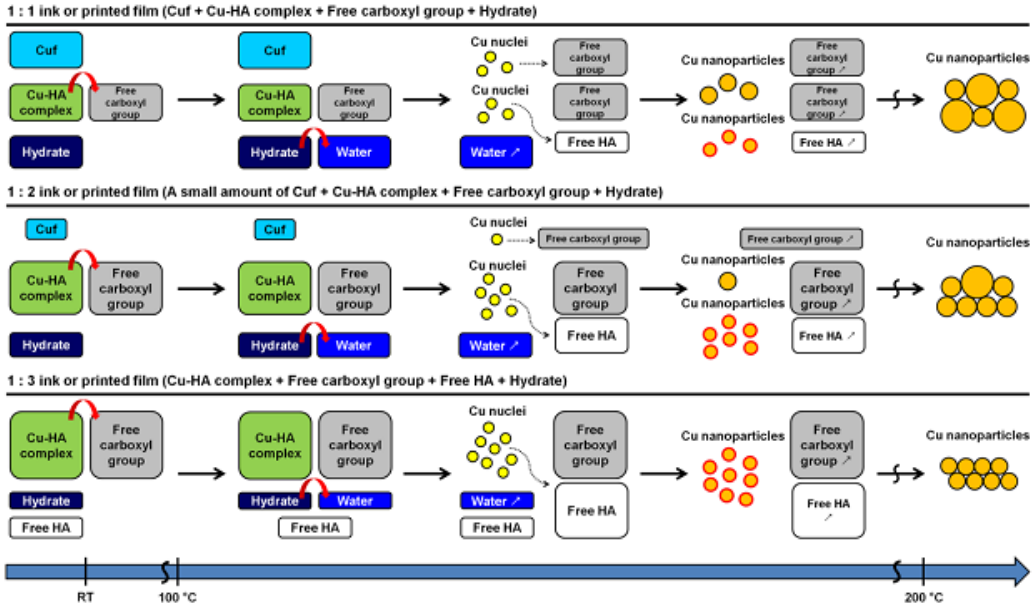

Fig. 1.8 Schematic diagram explaining microstructure formation during the thermal heating process with various amine concentrations in CuF-HA complex ink.[28]

Li *et al.* have printed conductive copper and nickel lines via a reactive inkjet printing process of a copper/nickel salt and a reducing agent from a multi-color printhead.[29] For printed copper lines, the best conductivity was 1.8×10^{6} S m^{-1}; that

of nickel is 2.2 × 10^4 S m^{-1}. EDS elemental analysis was used for analyze the oxidation of printed copper /nickel lines in air. It was found that inkjet printed nickel lines appeared to have less oxidation. This inkjet printing process can be used for other metals.

Flash light sintering

Dharmadasa and coworkers used an economically viable method for producing copper based conductive films on both flexible PET and glass substrates.[30] Intense pulsed light (IPL) technique has been used for sintering nanoparticles. In this study, synthesis of Cu/Cu_2O NP at room temperature, the ratio of Cu/Cu_2O, and IPL process parameters were optimized. For the synthesis of Cu/Cu_2O NP, adjusting the pH of the ink and the solvent/cosolvent were key factors. To control the ratio of Cu/Cu_2O, the concentration of the $NaBH_4$ was modulated. The IPL parameters were also optimized to generate Cu films with high electrical conductivity. The generated highly conductive Cu film had some Cu_2O phases. After applying 1723 J cm^{-2} to 10 cm^2 film, the lowest bulk resistivity of 9.40 × 10^{-7} Ω m was yielded (Fig. 1.9).

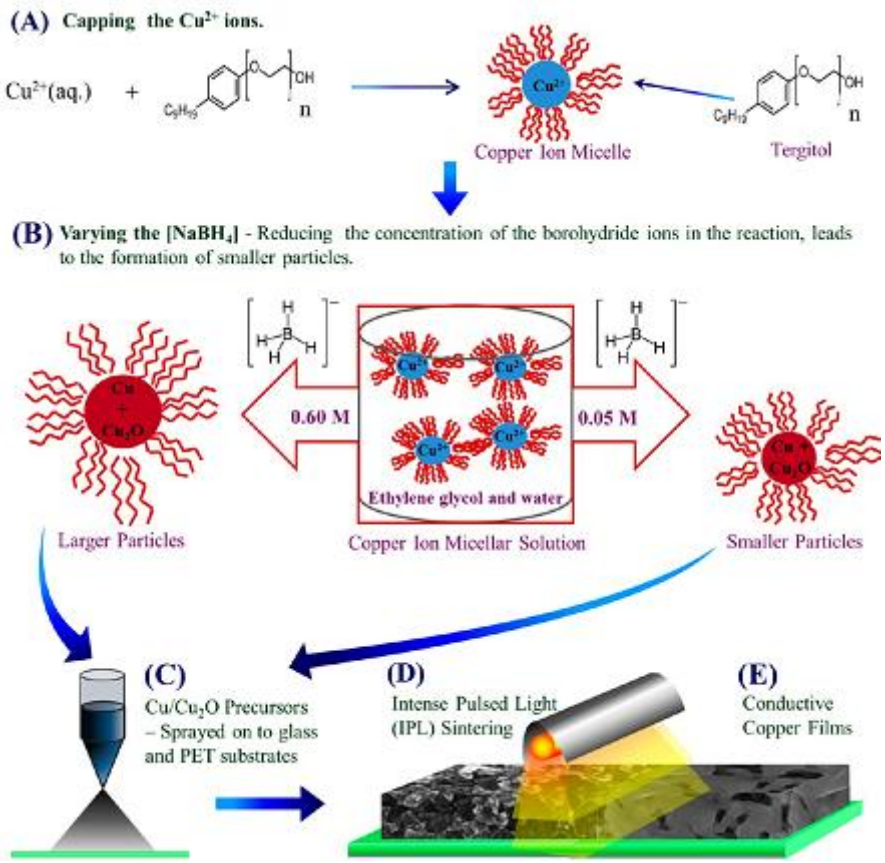

Fig. 1.9 Schematic illustration of the synthetic route for the preparation of the copper nanoparticle inks and the IPL sintering process of the ink.[30]

Kang and coworkers have converted CuO layers which were inkjet-printed on a porous PET substrate with primer coating to Cu by an IPL sintering process (Fig. 1.10).[31] The conductivity could reach up to 30% conductivity of bulk Cu. Insulating CuO layer was changed to conductive Cu within 6 ms without pre-drying process to evaporate solvents of the inks. The lowest resistivity of Cu layers using IPL sintering of 0.26 s was $5.5 \times 10^{-7}\ \Omega$ m, which was about 30% of bulk Cu conductivity.

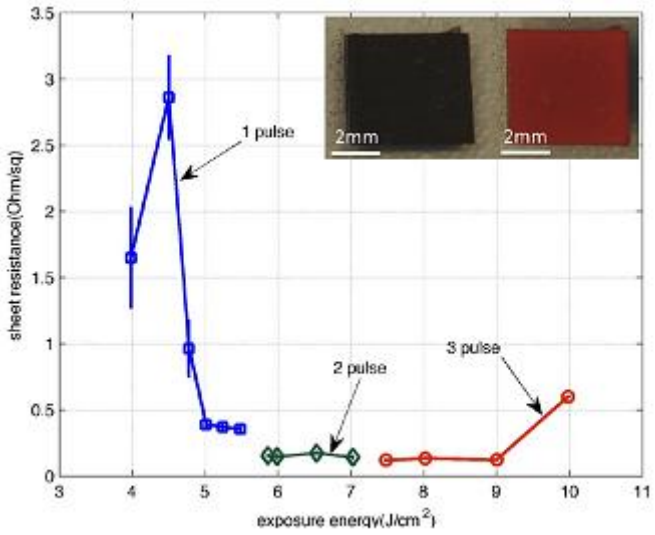

Fig. 1.10 Sheet resistance of Cu layer after IPL sintering *vs.* energy exposure and number of pulses. The pulse duration is 6 ms and the frequency for multi pulses is 10 Hz. The as-printed CuO (left) and IPL-sintered Cu (right) were also shown in the figure.[31]

1.3 Research target and approaches

1.3.1 Research target

The research target is to obtain the sintered copper films with high conductivities at low sintering temperatures (≤ 200 °C).

1.3.2 Approaches

About the approaches for achieving low resistivity of copper films at low sintering temperature, we have introduced several methods (decreasing particle size to nanoscale, using MOD ink, flash light sintering) in the above parts. In comparison, the reduction of the particle size may lead to easier oxidation, which results in problems with storage. Photonic sintering requires high-intensity pulsed light (HIPL)

irradiation equipment, which is expensive.

As mentioned above, decreasing particle size (<100 nm) can lead to easier oxidation of particles under an ambient atmosphere. In the second chapter, a new approach was proposed. Instead of using copper nanoparticles to facilitate the sintering, we firstly synthesized copper fine particles (~280 nm) and then utilized a facile thermal oxidation process to obtain copper film with low resistivity at low sintering temperature (200 ℃). It was proved that this thermal oxidation process can increase the contacts among particles and thus be beneficial to effective sintering of copper fine particles (>100 nm).

Third chapter presents an approach to obtain low temperature sintering based on a modified MOD inks using copper particles. Among the methods of low temperature sintering, using copper-based MOD inks is preferred because of its scalability and simplicity. In general, MOD inks consist of copper salts, ligands, and some organic components. In this study, conductive films with low resistivity after low temperature sintering were obtained by replacing the organic components in the MOD inks. In addition, several copper salts for the MOD ink were also compared. The above studies were shown in the third chapter.

In the fourth chapter, surface modification of the added copper particles was investigated to obtain conductive copper films based on the MOD inks with lower resistivity. The prepared MOD inks were composed of polydispersed-submicron copper particles which were stabilized with decomposable polymer (polypropylene carbonate, PPC) as a main part and a self-reducible copper

formate/1-amino-2-propanol (CuF-IPA) complex as an additive. The surface modification of copper particles with PPC, using of smaller polydispersed copper particles, and self-reducible copper complex contribute for achieving high conductivity of copper films at low sintering temperature.

Chapter 5 summarizes the obtained results and findings and gives general conclusions and perspective of the research presented in this thesis.

1.4 References

1 Nir, M. M.; Zamir, D.; Haymov, I.; Ben-Asher, L.; Cohen, O.; Faulkner, B.; De La Vega, F. *The Chemistry of Inkjet Inks* (Ed.: S. Magdassi); World Scientific, New Jersey, London, Singapore, 2010.

2 Cummins, G.; Desmulliez, M. P. Y. *Circuit Wor*; Emerald Group Publishing, Ltd.: W Yorkshire, England, 2012.

3 Yoshioka, Y.; Jabbour, G. E. Desktop Inkjet Printer as a Tool to Print Conducting Polymers. *Synth. Met.* **2006**, *156*, 779-783.

4 Shrotriya, V. Organic Photovoltaics: Polymer Power. *Nat. Photonics* **2009**, *3*, 447-449.

5 Hilder, M.; Winther-Jensen, B.; Clark, N. B. Paper-Based, Printed Zinc–Air Battery. *J. Power Sources* **2009**, *194*, 1135-1141.

6 Subramanian, V.; Fréchet, J. M. J.; Chang, P. C.; Huang, D. C.; Lee, J. B.; Molesa, S. E.; Murphy, A. R.; Redinger, D. R.; Volkman, S. K. Progress Toward Development of All-Printed RFID Tags. Materials, Processes, and Devices. *Proc. IEEE* **2005**, *93*, 1330-1338.

7 Song, K.; Kim, D.; Li, X. S.; Jun, T.; Jeong, Y.; Moon, J. Solution Processed Invisible All-Oxide Thin Film Transistors. *J. Mater. Chem.* **2009**, *19*, 8881-8886.

8 Leenen, M. A. M.; Arning, V.; Thiem, H.; Steiger, J.; Anselmann, R. Printable Electronics: Flexibility for the Future. *Phys. Status Solidi A* **2009**, *206*, 588-597.

9 Kamyshny, A.; Magdassi, S. Conductive Nanomaterials for Printed Electronics. *Small* **2014**, *10*, 3515-3535.

10 http://www.metalprices.com, accessed 20th January 2010.

11 Groenendaal, L. B.; Jonas, F.; Freitag, D.; Pielartzik, H.; Reynolds, J. R. Poly(3,4-ethylenedioxythiophene) and Its Derivatives: Past, Present, and Future. *Adv. Mater.* **2000**, *12*, 481-494.

12 Park, S.; Vosguerichian, M.; Bao, Z. A Review of Fabrication and Applications of Carbon

Nanotube Film-Based Flexible Electronics. *Nanoscale* **2013**, *5*, 1727-1752.

13 Tickle, A. C. *Thin-Film Transistor: A New Approach to Micrelectronics*; Wiley: New York, 1999.

14 de Leeuw, D. M.; Simenon, M. M. J.; Brown, A. R.; Einhard, R. E. F. Stability of n-Type Doped Conducting Polymers and Consequences for Polymeric Microelectronic Devices. *Synth. Met.* **1997**, *87*, 53-59.

15 Martins, R.; Ferreira, I.; Fortunato, E. Electronics with and on Paper. *Phys. Status Solidi: Rapid Res. Lett.* **2011**, *5*, 332-335.

16 Singh, M.; Haverinen, H. M.; Dhagat, P.; Jabbour, G. E. Inkjet Printing - Process and Its Applications. *Adv. Mater.* 2010, *22*, 673-685.

17 Wünscher, S.; Abbel, R.; Perelaer, J.; Schubert, U. S. Progress of Alternative Sintering Approaches of Inkjet-Printed Metal Inks and their Application for Manufacturing of Flexible Electronic Devices. *J. Mater. Chem. C* **2014**, 2, 10232-10261.

18 Moon, K. S.; Dong, H.; Maric, R.; Pothukuchi, S.; Hunt, A.; Li, Y.; Wong, C. P. Thermal Behavior of Silver Nanoparticles for Low-Temperature Interconnect Applications. *J. Electron. Mater.* **2005**, *34*, 168-175.

19 Buffat, P.; Borel, J. Size Effect on the Melting Temperature of Gold Particles. *Phys. Rev. A* **1976**, *13*, 2287-2298.

20 Yang, C.; Wong, C. P.; Yuen, M. M. F. Printed Electrically Conductive Composites: Conductive Filler Designs and Surface Engineering. *J. Mater. Chem. C* **2013**, *1*, 4052-4069.

21 Deng, D.; Jin, Y.; Cheng, Y.; Qi, T.; Xiao, F. Copper Nanoparticles: Aqueous Phase Synthesis and Conductive Films Fabrication at Low Sintering Temperature. *ACS Appl. Mater. Interfaces* **2013**, *5*, 3839-3846.

22 Hokita, Y.; Kanzaki, M.; Sugiyama, T.; Arakawa, R.; Kawasaki, H. High-Concentration Synthesis of Sub-10-nm Copper Nanoparticles for Application to Conductive Nanoinks. *ACS Appl. Mater. Interfaces* **2015**, *7*, 19382-19389.

23 Sugiyama, T.; Kanzaki, M.; Arakawa, R.; Kawasaki, H. Low-Temperature Sintering of Metallacyclic Stabilized Copper Nanoparticles and Adhesion Enhancement of Conductive Copper Film to a Polyimide Substrate. *J. Mater. Sci.: Mater. Electron.* 2016; DOI: 10.1007/s10854-016-4734-8.

24 Shin, D.-H.; Woo, S.; Yem, H.; Cha, M.; Cho, S.; Kang, M.; Jeong, S.; Kim, Y.; Kang, K.; Piao, Y. A Self-Reducible and Alcohol-Soluble Copper-Based Metal-Organic Decomposition Ink for Printed Electronics. *ACS Appl. Mater. Interfaces* **2014**, *6*, 3312-3319.

25 Farraj, Y.; Grouchko, M.; Magdassi, S. Self-Reduction of a Copper Complex MOD Ink for Inkjet Printing Conductive Patterns on Plastics. *Chem. Commun.* **2015**, *51*, 1587-1590.

26 Kim, S. J.; Lee, J.; Choi, Y.-H.; Yeon, D.-H.; Byun, Y. Effect of Copper Concentration in

Printable Copper Inks on Film Fabrication. *Thin Solid Films* 2012, *520*, 2731-2734.

27 Yabuki, A.; Tanaka, S. Electrically Conductive Copper Film Prepared at Low Temperature by Thermal Decomposition of Copper Amine Complexes with Various Amines. *Mater. Res. Bull.* **2012**, *47*, 4107-4111.

28 Choi, Y.-H.; Hong, S.-H. Effect of the Amine Concentration on Phase Evolution and Densification in Printed Films Using Cu (II) Complex Ink. *Langmuir* **2015**, *31*, 8101-8110.

29 Li, D.; Sutton, D.; Burgess, A.; Graham, D.; Calvert, P. D. Conductive Copper and Nickel Lines via Reactive Ink Jet Printing. *J. Mater. Chem.* **2009**, *19*, 3719-3724.

30 Dharmadasa, R.; Jha, M.; Amos, D. A.; Druffel, T. Room Temperature Synthesis of a Copper Ink for the Intense Pulsed Light Sintering of Conductive Copper Films. *ACS Appl. Mater. Interfaces* **2013**, *5*, 13227-13234.

31 Kang, H.; Sowade, E.; Baumann, R. R. Direct Intense Pulsed Light Sintering of Inkjet-Printed Copper Oxide Layers within Six Milliseconds. *ACS Appl. Mater. Interfaces* **2014**, *6*, 1682-1687.

2. Two-Step Annealing Process of Copper Fine Particles towards Improving Electrical Conductivity of Copper Films at Low Sintering Temperature

2.1 Introduction

Reducing particle size as a common method to facilitate the sintering of copper particles at low sintering temperatures suffers from the problems of copper nanoparticle (less than 100 nm) oxidation during storage and complicated synthesis process which usually use an inert gas. Copper fine particles can be stored much more easily compared with copper nanoparticles. However, it is well acknowledged that the larger the particle is, the more difficult the particle can be sintered due to the lower chemical potential.

To solve the above problems, a facile thermal oxidation process which can generate nanostructures and thus increase the contact between particles was introduced. Nanorods or nanowire-like copper oxides generated via a thermal oxidation process[1-4] have been extensively reported for the wide application in gas sensors,[5] heterogeneous catalysts,[6] etc. To the best of our knowledge, this is the first time to take advantage of nanorods or nanowire-like structure to facilitate the coalescence of copper particles. Ida and coworker have demonstrated that an oxidative preheating process in air can be used to remove the capping layers on copper nanoparticles[7] and exhibited that the thermal oxidative preheating process was

pivotal in obtaining conductive films with a high conductivity.[8] But it is still not clear about the mechanism of this oxidative preheating process. Some studies used an *In-situ* TEM to observe the structural changes of copper fine particles with and without air, but it is still difficult for the complete understanding.[7,9]

In this work, a new route for improving the conductivity of copper film was proposed. It can be achieved by a two-step process. In the first step, copper fine particles were synthesized by using D-isoascorbic acid as the mild reductant and octylamine as the capping agent. In the second step, an oxidative preheating process was used to generate convex surfaces, nanorods or nanoparticles successfully and thus to facilitate the coalescence of particles, leading to high conductivity of copper films after sintering process. To our best knowledge, this is our first time to demonstrate that the oxidative preheating process can improve the sintering behavior of particles by producing nanorods or nanoparticles. The mechanism of oxidative preheating process and its influence on the conductivity of obtained copper films were investigated. The results indicate that prepared copper films have high electrical conductivity owing to the roles of oxidative preheating process on the following reductive sintering process.

2.2 Experimental section

2.2.1 Synthesis of copper fine particles

The synthetic procedure presented in this work is illustrated in Fig. 2.1.

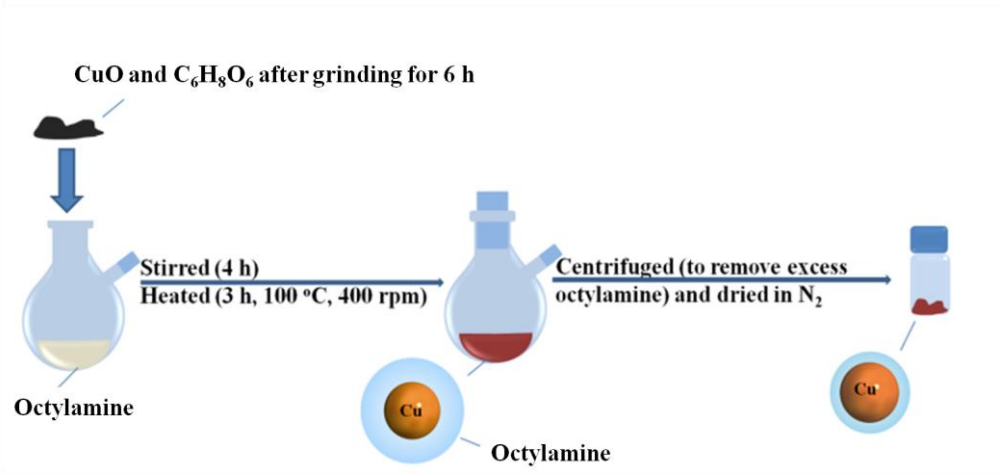

Fig. 2.1 Schematic illustration of one-pot synthesis of copper fine particles.

For the preparation of copper fine particles, copper oxide (CuO, agglomerates with size ranging from a few hundred nanometers to several micro-meters, Nissin Chemco, Kyoto Japan), D-isoascorbic acid ($C_6H_8O_6$, 98%, Acros) agent, octylamine (98%, Wako, Japan or Lion Corp.) and α-terpineol (95%, Kanto, Japan) were chosen as the copper precursor, reducing agent, capping agent and dispersing agent, respectively. CuO (2.5 g, 31 mmol) and $C_6H_8O_6$ (5.5 g, 31 mmol) were grinded for 6 h using a mortar and then dissolved in octylamine (52 ml, 310 mmol) in a two-neck round-bottom flask which was equipped with a condenser and a stirring bar. The prepared mixture was heated at 100 ℃ for 3 h with a stirring speed of 400 rpm using an oil bath after mixing for 4 h using a magnetic stirrer. After that, ethyl acetate was used to centrifuge and wash the mixture (10,000 rpm, 30 min). This centrifugation process was carried out for several times and dried under a nitrogen flow to prepare copper A sample. According to the low solubility of protonated octylamine[10] (with the combination of proton derived from ascorbic acid, some octylamine changed to

protonated octylamine) in methanol, copper fine particles with much protonated octylamine (copper B, in Fig. 2.2) were also got using the same preparation method after centrifugation with methanol for three times and drying under a nitrogen gas.

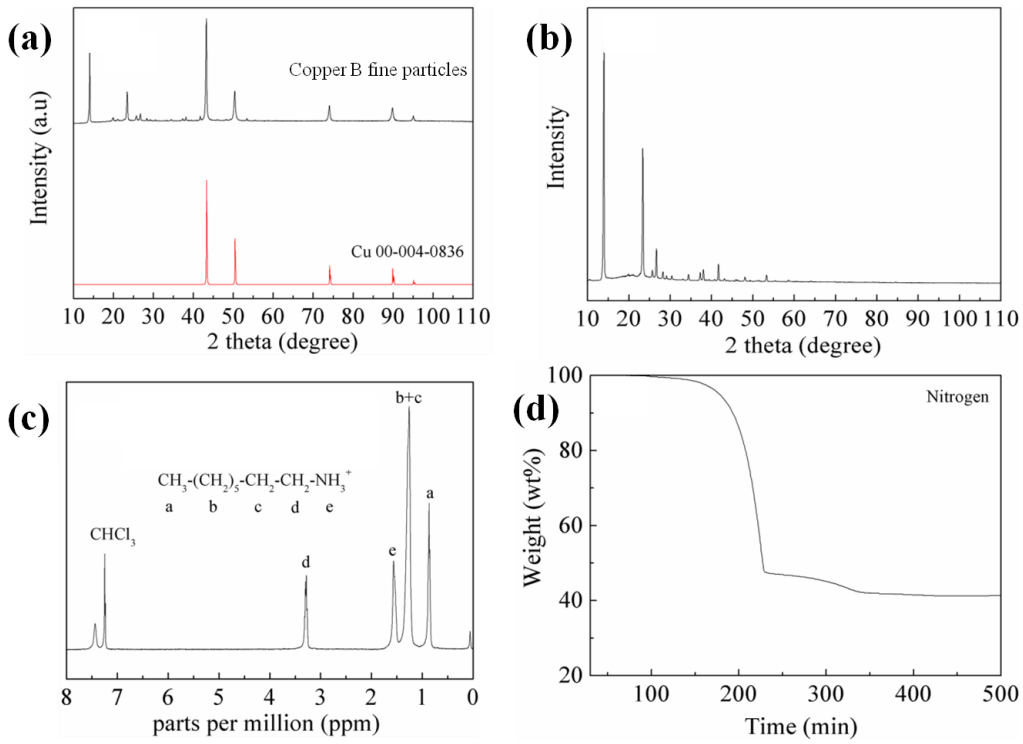

Fig. 2.2 XRD patterns of (a) copper B fine particles which contain much protonated octylamine and (b) Protonated octylamine. (c) NMR spectra of protonated octylamine. (d) TG curves of copper B fine particles in nitrogen.

2.2.2 Preparation of copper particle inks and films

After grinding with an automatic mortar for 30 min and pulverizing with a blender for 4 min, 30 wt% synthesized copper A fine particles were dispersed into 70 wt% of α-terpineol to prepare copper A inks. In addition, ethanol was also added into the dispersion for assisting redispersion of copper A particles. Then, the dispersion of copper A fine particles in α-terpineol was mixed by a conditioning mixer for 32 min

and by an emulsifier for 5 times. Finally, the copper A fine particle inks were prepared using evaporation under reduced pressure to remove ethanol from the dispersion. The obtained copper A fine particle inks were deposited on both aluminum oxide (Al_2O_3) (for resistivity measurements) and glass (for X-ray diffraction (XRD) measurements) slides using a doctor blade. The thicknesses of sintered films at 200 ℃, 250 ℃ and 300 ℃ which were measured using the cross section SEM images were 4.4, 4.6, and 3.4 μm, respectively (Fig. 2.3). Following drying under a nitrogen flow at 60 ℃ for 1 h, the copper films deposited on Al_2O_3 and glass substrates were cut to 2 cm × 2 cm pieces and annealed via a two-step process. During this two-step process as show in Fig. 2.4, the substrates deposited with copper A fine particle film were heated with a flow rate of 2 dm^3 min^{-1} under air for 4 h and sintered under a 3 % hydrogen-containing nitrogen gas with a flow rate of 2 dm^3 min^{-1} of for 3 h. The annealing temperature was kept at 200 ℃, 250 ℃ or 300 ℃. In addition, to observe the surface morphological changes of the copper A fine particles during the oxidative preheating process, copper A films were only heated in air without sintering procedure at various temperatures (200 ℃ and 250 ℃) for various periods (5 min, 30 min, 2 h and 4 h) with a flow rate of 2 dm^3 min^{-1} of air.

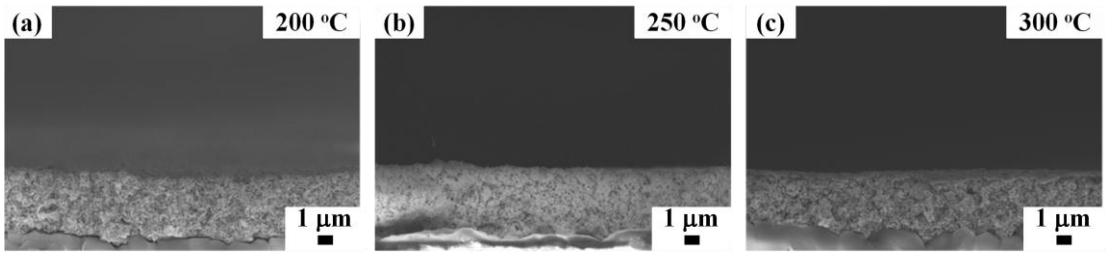

Fig. 2.3 The thicknesses of copper A films after annealing at various temperatures through a two-step process.

Prepared copper B fine particles which containing much protonated octylamine were also used for preparing the copper B inks and films with the above method. After that, the prepared copper B films were heated at 250 ℃ with an air flow under the same flow rate for various time (5 min, 30 min, 2 h and 4 h).

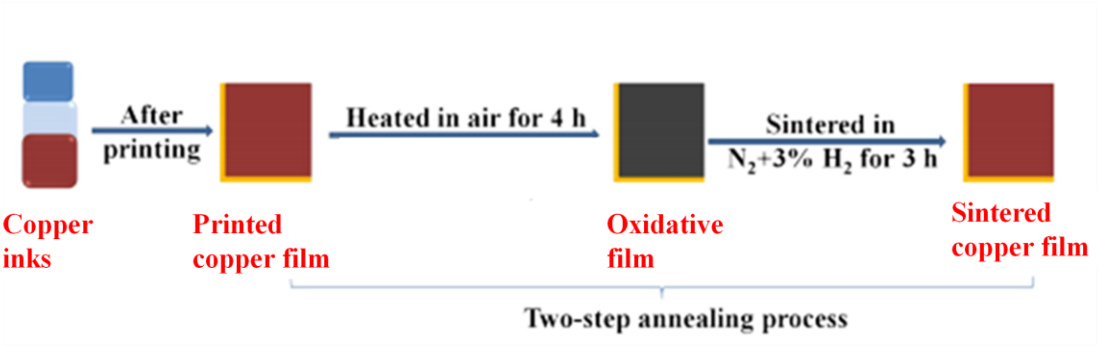

Fig. 2.4 Schematic illustration of two-step annealing process consisting of oxidative preheating process in air for 4 h (to enhance particle coalescence by generating convex surfaces, nanorods or nanoparticles) and sintering with a reductive gas containing 3% hydrogen-containing nitrogen gas for 3 h. The temperature in this two-step annealing process was kept for 200 ℃, 250 ℃ or 300 ℃.

2.2.3 Characterizations

X-ray Diffraction (XRD, a Rigaku Mini Flex II, Cu Kα) was used to analyze the crystal structures of prepared copper A fine particles and copper A films. A field emission scanning electron microscope (FE-SEM, JEOL JSM-6701F) at an accelerated voltage of 15 Kv was used for observing the morphologies of the copper A fine particles and the copper A films. The cross-sectional SEM images of the obtained conductive copper films were got to measure the thickness of films for calculating the volume resistivity of films. A four point probe method (Loresta-GP, MCP-T610,

Mitsubishi Chemical Analytech, Japan) was for measuring the sheet resistances of copper films.

For the copper B fine particles, thermogravimetric analysis (TG, SHIMADZU DTG-60H) were taken for the thermal property. In addition, the copper B films were also characterized by SEM, XRD, and resistivity measurements.

2.3 Results and discussion

Copper fine particles were prepared using a facile one-pot synthetic process (Fig. 2.1). Fig. 2.5 presents the SEM image and XRD pattern of obtained copper A fine particles. The size of prepared copper fine particles, which was measured by calculating 100 copper A fine particles statistically, was in the range of 130 nm to 300 nm with an average diameter of 280 nm. There are five characteristic peaks at 43.3 °, 50.4 °, 74.1 °, 89.9 °, and 95.1 ° as shown in XRD pattern (Fig. 2.5b), which are corresponding to (111), (200), (220), (311), and (222) planes of copper crystallites, respectively. In addition, no copper oxides in the copper A fine particles were detected according to XRD pattern (Fig. 2.5b). These can be ascribed to the role of octylamine which can act as an anti-oxidation agent by maintaining a reducing atmosphere during the reaction process and protecting the particles to be free of oxidation by absorbing onto the surfaces of copper particles.[10,11] In general, strong reducing agent like hydrazine,[7] and sodium borohydride,[12] and an inert gas are used for the synthesis of copper fine particles and nanoparticles. In contrast, copper fine particles prepared in this work were prepared with a mild reducing agent and ambient atmosphere.

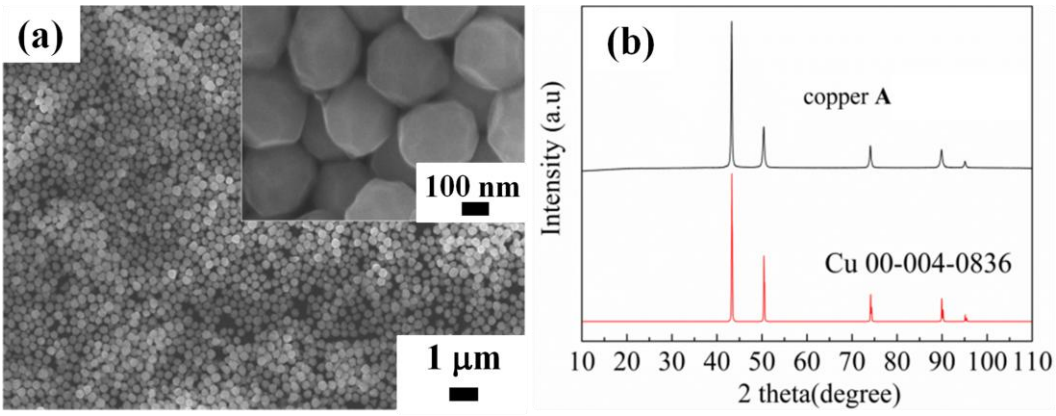

Fig. 2.5 (a) Morphologies and (b) XRD pattern of copper A fine particles.

To study the oxidative preheating process, copper A films were preheated in air for various periods at 200 ℃. Fig. 2.6 displays the SEM images and XRD patterns of copper A films oxidatively preheated for various heating periods (0 min, 5 min, 30 min, 2 h, and 4 h) at 200 ℃. Before the oxidatively preheating process, the surfaces of copper A fine particles which are separated by the octylamine layers are smooth as displayed in Fig. 2.6a. These smooth surfaces indicate that obvious oxidation of the surfaces of copper A fine particle did not occur, which was identical to the result of XRD pattern (Fig. 2.6f). When the preheating time increased to 5 min, it can be observed that particles shows obvious coalescence caused by the generated convex surfaces (Fig. 2.6b). Coalescence of particles and tight connections of particles also happened when the preheating time were 30 min, 2 h, and 4 h (Figs. 2.6b-2.6e). With the combination of XRD results as presented in Fig. 2.6f, the above generated convex surfaces are corresponding to cuprous oxide (Cu_2O) resulted from the oxidation of metallic copper.

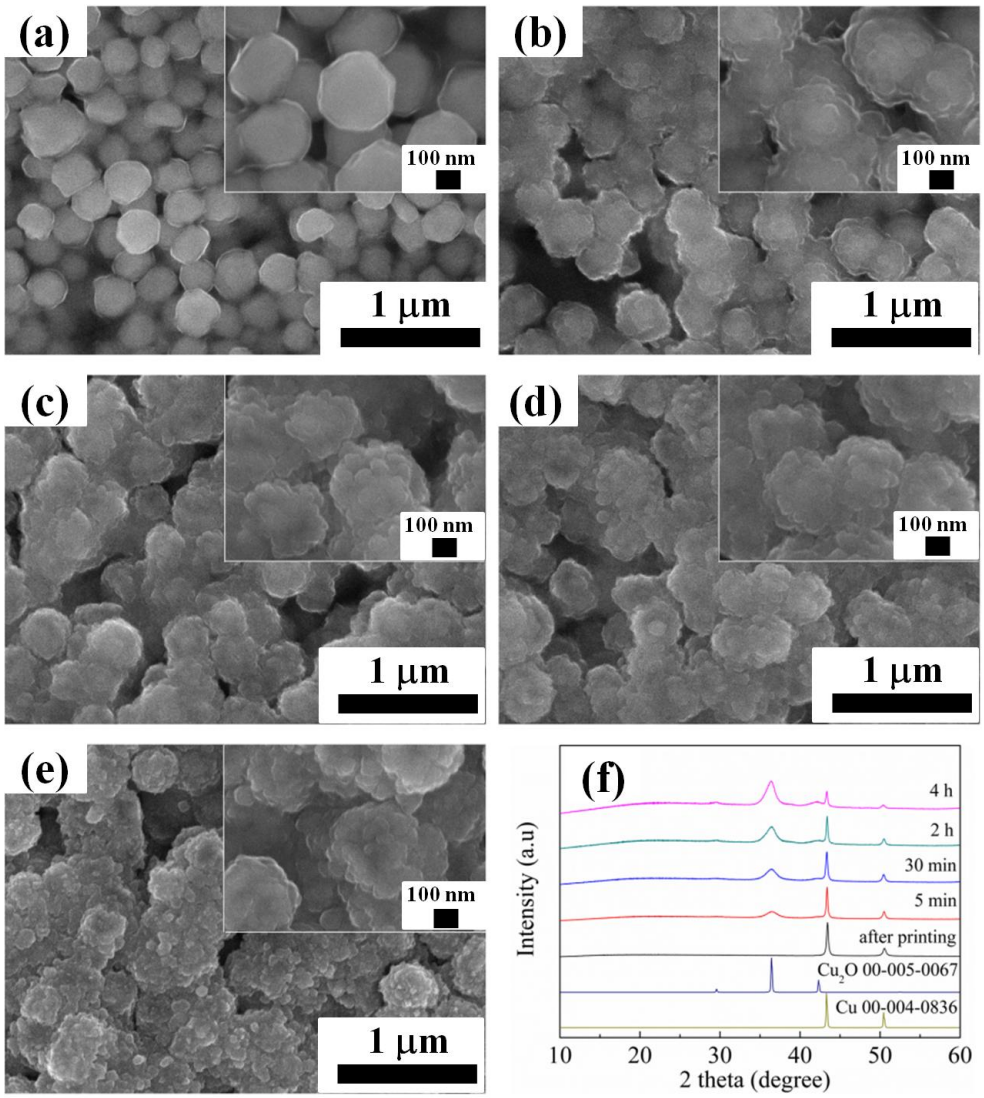

Fig. 2.6 Morphological images of copper A films after oxidative preheating at for various periods 200 ℃: (a) 0 min, (b) 5 min, (c) 30 min, (d) 2 h, and (e) 4 h. (f) X-ray diffraction patterns.

The morphological changes of copper A films after oxidative preheating process for various heating time at 250 ℃ are exhibited in Figs. 2.7a-2.7d. When the preheating time changes from 5 min to 4 h, generated convex surfaces and coalescence of fine particles, which are same as the phenomena of copper A films after oxidative preheating process at 200 ℃, can also be observed (Figs. 2.7a-2.7d). Furthermore, nanorods which can result in the generation of denser films also

appeared (Figs. 2.7b-2.7d).

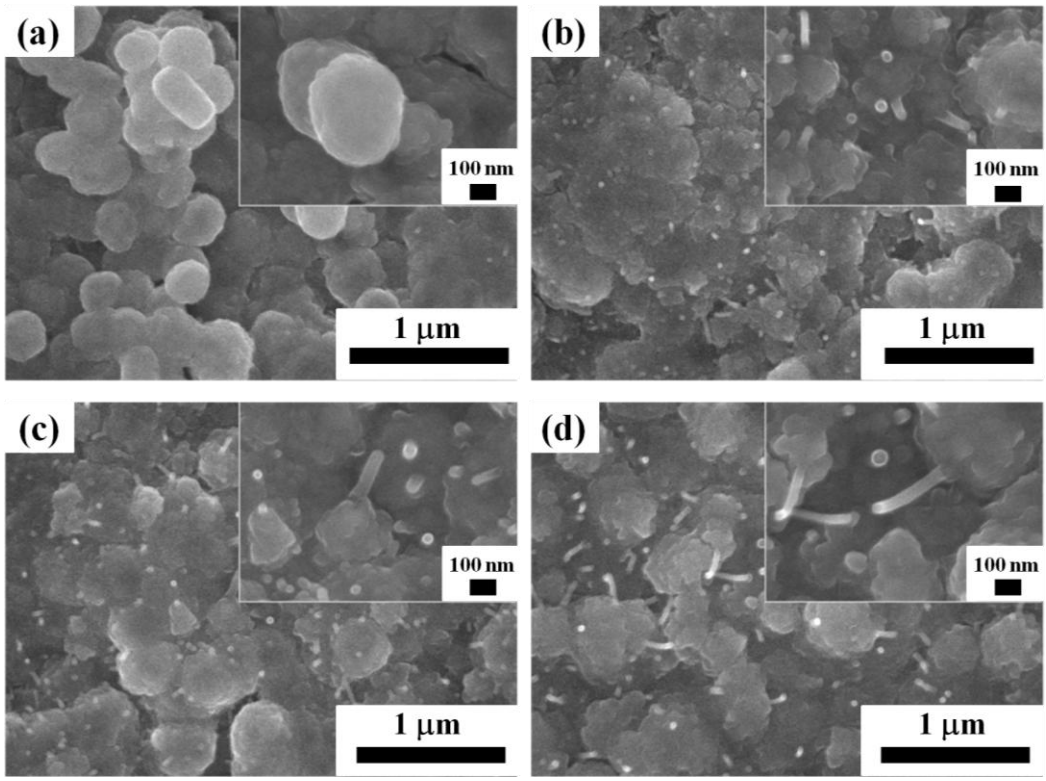

Fig. 2.7 Morphological images of copper A films after oxidative preheating at 250 ℃ for various periods: (a) 5 min, (b) 30 min, (c) 2 h, and (d) 4 h.

Fig. 2.8 exhibits the XRD results of copper A films after oxidative preheating process for various heating time at 250 ℃. After oxidative preheating for 5 min, copper fine particles were oxidized to Cu_2O and small amounts of CuO. The intensity of metallic copper peaks decreased with the increase of oxidative preheating time. After oxidative sintering for 2 h, all the metallic copper was changed to copper oxides. Based on the above results and corresponding SEM images (Figs. 2.7a-2.7d), it can be found that copper oxides which include Cu_2O or CuO result in the formation of convex surfaces generated at the beginning of oxidative preheating process and nanorods with the continuing of the oxidation process.

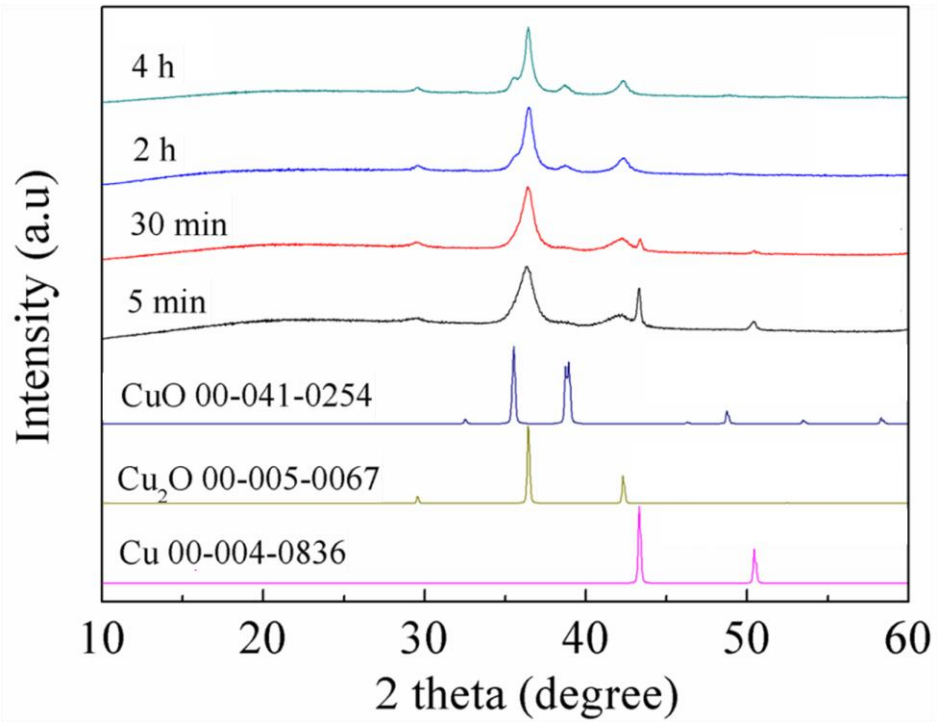

Fig. 2.8 X-ray diffraction patterns of copper A films after oxidative preheating process at 250 ℃ for various heating time (5 min, 30 min, 2 h, 4 h).

The oxidative process of copper B films prepared using copper B fine particles which containing much protonated octylamine was also carried out at 250 ℃. Interestingly, smaller nanoparticles not nanorods appeared on the surface of particles (Figs. 2.9c-2.9e). The XRD results (Figs. 2.9f) also present different results compared with that of copper A films after oxidative preheating at 250 ℃ (Fig. 2.8). When the oxidative preheating time were 5 and 30 min, the peaks representing metallic copper, Cu_8O and Cu_2O can be detected. When the oxidative preheating time extended to 2 and 4 h, the peaks related to Cu_8O, Cu_2O and CuO coexisted in the obtained films. Besides the well-known copper oxides such as Cu_2O and CuO, there are other

metastable phases like Cu_8O,[13] $Cu_{64}O$,[14] etc, which are formed in certain atomic diffusion depth.

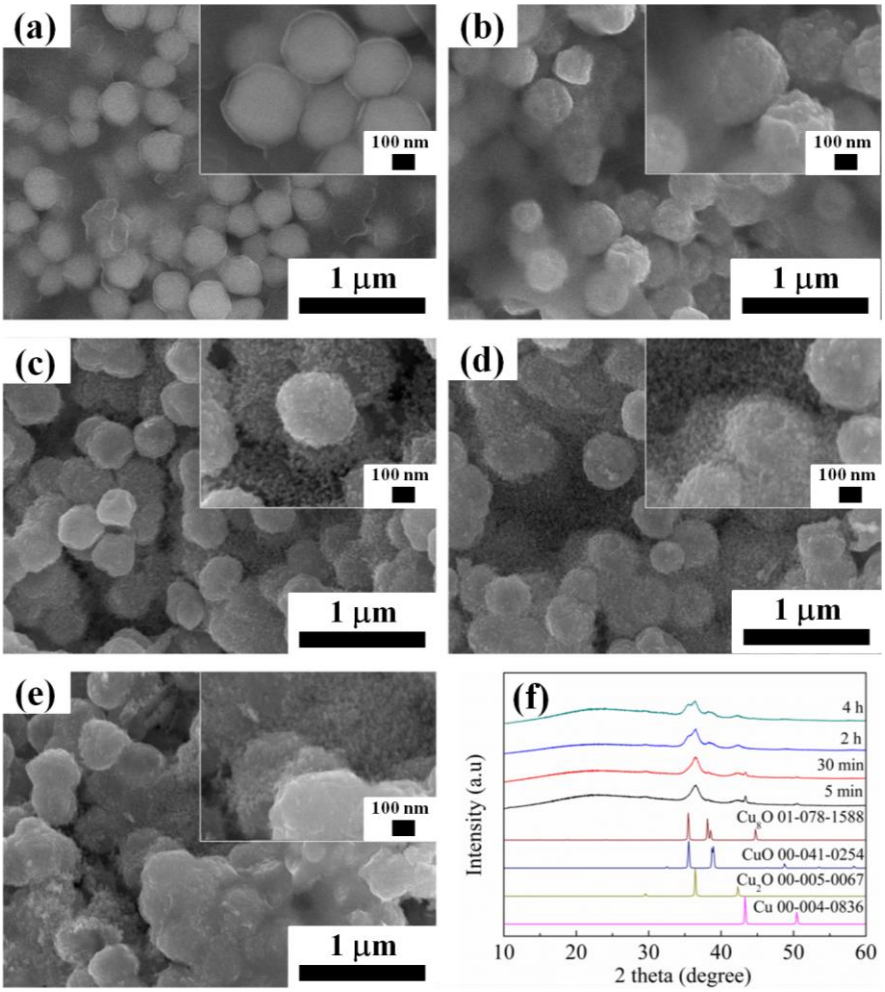

Fig. 2.9 SEM of copper B films after oxidative preheating process at 250 ℃ for various heating periods: (a) 0 min, (b) 5 min, (c) 30 min, (d) 2 h, and (e) 4 h. (f) Corresponding XRD patterns.

Fig. 2.10 expressed the mechanism of the oxidative preheating process. During the oxidative preheating process, there are two main reaction which are shown by the the following equations.

$$4Cu + O_2 \longrightarrow 2Cu_2O \quad (1)$$

$$2Cu_2O + O_2 \longrightarrow 4CuO \quad (2)$$

The oxidative preheating process includes the diffusion of copper ion from the copper matrix to the film surface[2,15] and oxygen.[16] It involves two stages. In the first stage, convex surfaces are formed owing to the diffusion of oxygen and copper ion as shown in Figs. 2.6b-2.6e, 2.7a and 2.9b. The generated products strongly depend on the oxidative temperature. If the oxidative temperature is low (200 ℃), metallic copper was only be oxidized to Cu_2O according to eq. 1. If the oxidative temperature is high enough (250 or 300 ℃), partially formed Cu_2O can act as a catalyst and transform into CuO (eq. 2).[3,17] For copper B fine particles which are surrounded by plenty of protonated octylamine, Cu_8O which was detected in XRD (Fig. 2.9f) can be formed due to the limited contact between oxygen and copper ion caused by too much protonated octylamine. For the second stage, nanorods (Figs. 2.7b-2.7d) or formation of nanoparticles (Figs. 2.9c-2.9e) were generated. Vapour-liquid-solid (VLS),[18] vapour-solid (VS),[19] or diffusion mechanism.[4,15] are frequently used to explain the mechanism of nanorods or nanowires generated by thermal oxidation process. The VLS mechanism needs catalyst and droplet on the top of nanowires or nanorods can be found. For the VS mechanism, the temperatures used during this oxidative preheating process are much lower than the melting point of metallic copper and copper oxides.[2] The plausible reason for the generation and growth of nanorods are that the local electric field which is set up by the oxygen ions at the solid/gas interface can improve the diffusion of the oxygen ions and copper ions[3] and chemical reactions between oxygen ions and copper ion occur. The generation of both Cu_2O and CuO (eqs. 1 and 2) can only occur at a high oxidative preheating temperature (250 or

300 ℃). When the copper fine particles are surrounded by lots of protonated octylamine, the electrostatic force can interfere with the electric field and thus have an effect on the diffusion of copper ion to form nanorods which grow by copper ion from the initial nuclear site to the top, leading to the small nanoparticles. In addition, metastalble Cu_8O, CuO and Cu_2O can coexist in the formed films due to protonated octylamine.

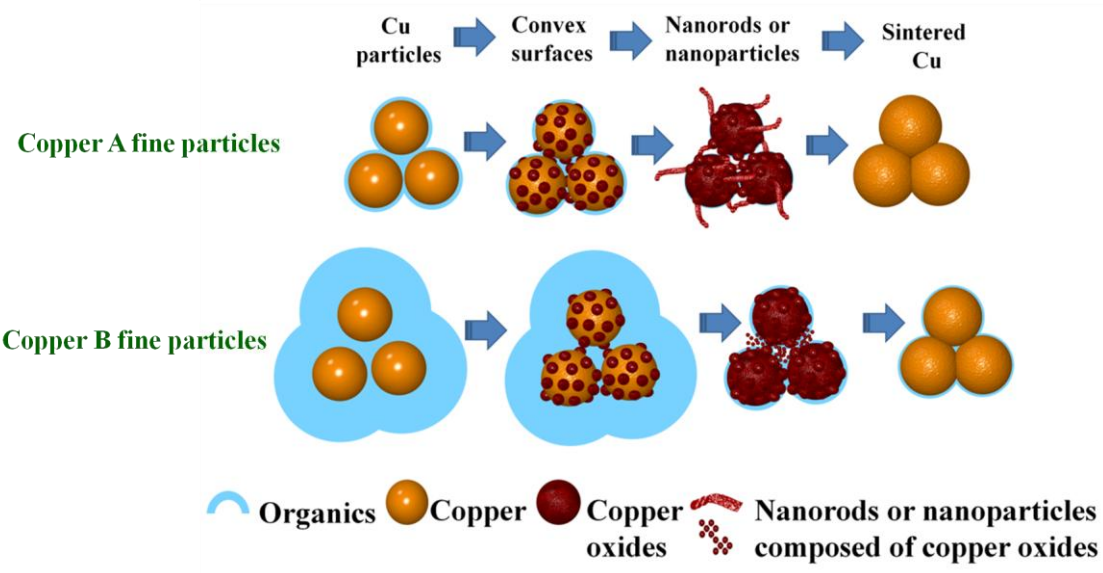

Fig. 2.10 Schematic diagram of the oxidative preheating process during which convex surfaces, nanorods or nanoparticles can be generated and consequently facilitate the particle sintering.

Copper A films after oxidative preheating in air for 4 h (Figs. 2.11a, 2.11c and 2.11e) and copper A films (Figs. 2.11b, 2.11d and 2.11f) after two step annealing process at 200 ℃, 250 ℃ and 300 ℃ can be shown in Fig. 2.11. According to the SEM images of copper films after oxidative preheating process at 200 ℃, 250 ℃ and 300 ℃ for 4 h, the coalescence among particles and compact films can be obvious observed. Furthermore, the higher the oxidative preheating temperature was, the

denser the generated oxidative film was (Figs. 2.11a, 2.11c and 2.11e). Following the reductive sintering process under a mixture of N_2 and H_2 gas at various temperatures, highly compact copper films reduced from the oxidative films with less cracks were formed (Figs. 2.11b, 2.11d, 2.11f and 2.12). Moreover, denser copper film were obtained at higher reducing temperature. The resistivities of copper A films after two-step annealing process are exhibited in Fig. 2.13. The copper A films after two-step annealing process at 200 ℃, 250 ℃ and 300 ℃ can achieve low resistivities of 1.2×10^{-7}, 7.8×10^{-8} and 5.6×10^{-8} Ω m, respectively. The electrical resistivity decreases with the two-step annealing temperature increases, which are consistent with the morphological images as shown in Figs. 2.11b, 2.11d and 2.11f. The resistivity of copper A film after two-step annealing process at 200 ℃ is just 7 times of that of bulk copper (1.7×10^{-8} Ω m). This excellent electrical conductivity of obtained copper films can be ascribed to the important role of thermal oxidative preheating process. Convex surfaces generated during the preheating process are favorable to the tight connections among adjacent particles. Nanorods can grow toward various directions and thus cause further tight connection of particles and formation of denser network structures. Consequently the particles sintering were greatly facilitated. Copper B films which even contain lots of organics also achieved relatively low resistivities of 8.2×10^{-7} and 8.6×10^{-7} Ω m at 250 ℃ and 300 ℃, respectively (Fig. 2.14). These are due to the effects of generated small oxide nanoparticles during thermal oxidative preheating process. It is well known that small nanoparticles can enhance the particle sintering.[20] Moreover, these generated oxide

nanoparticles in this study can facilitate particle sintering by provide close contacts between particles. At last, after reductive sintering process, annealed copper films with low resistivity were obtained with the help of convex surfaces, oxide nanorods or oxide nanoparticles (Fig. 2.10).

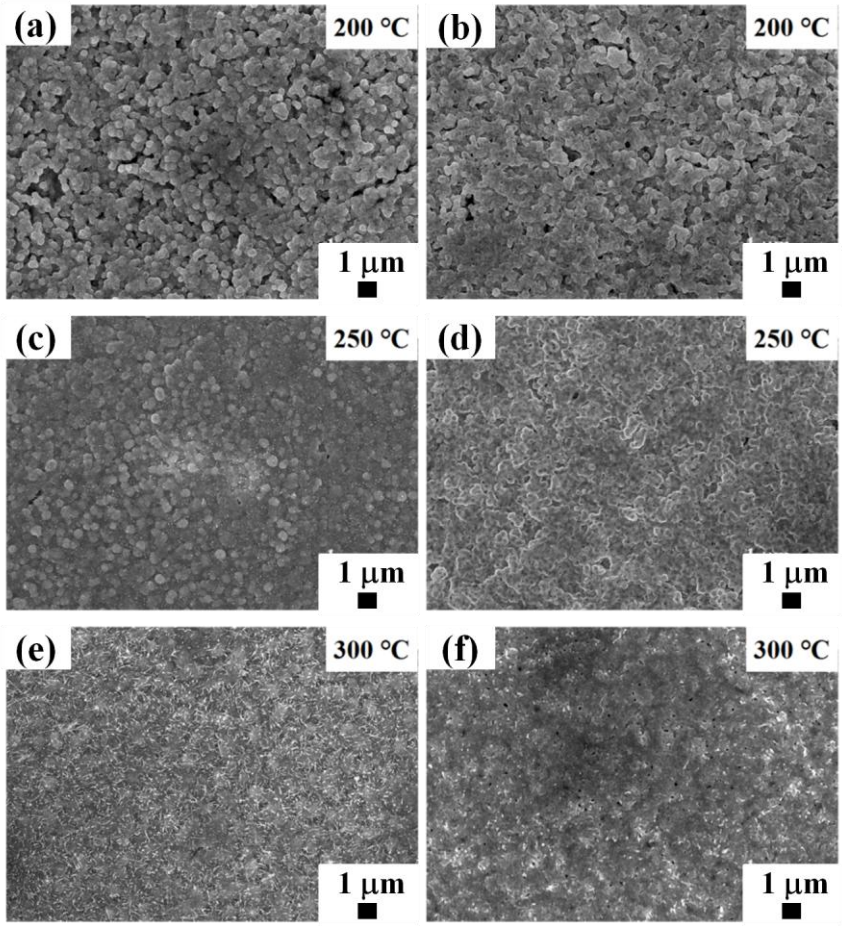

Fig. 2.11 Morphological changes of copper A films after oxidative preheating process in air for 4 h (a, c and e) and copper A films after two-step annealing process including thermal oxidative preheating process in air for 4 h and following reductive sintering process in nitrogen with 3 % hydrogen gas for 3 h at 200 ℃, 250 ℃ and 300 ℃, respectively (b, d and f).

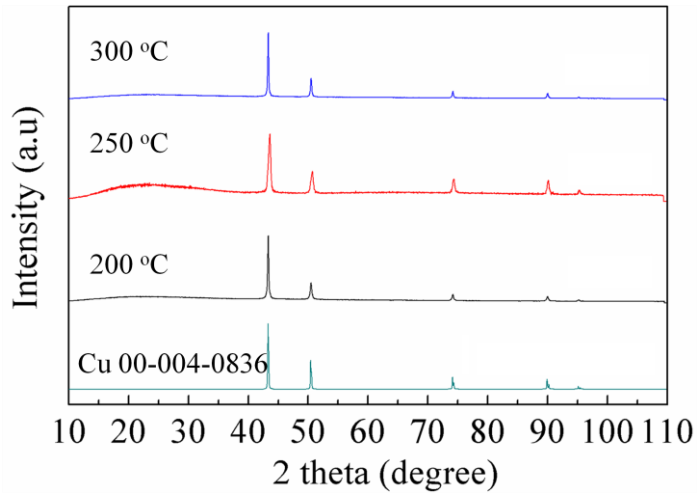

Fig. 2.12 XRD patterns of copper A films after two-step annealing process at 200 ℃, 250 ℃ and 300 ℃, respectively.

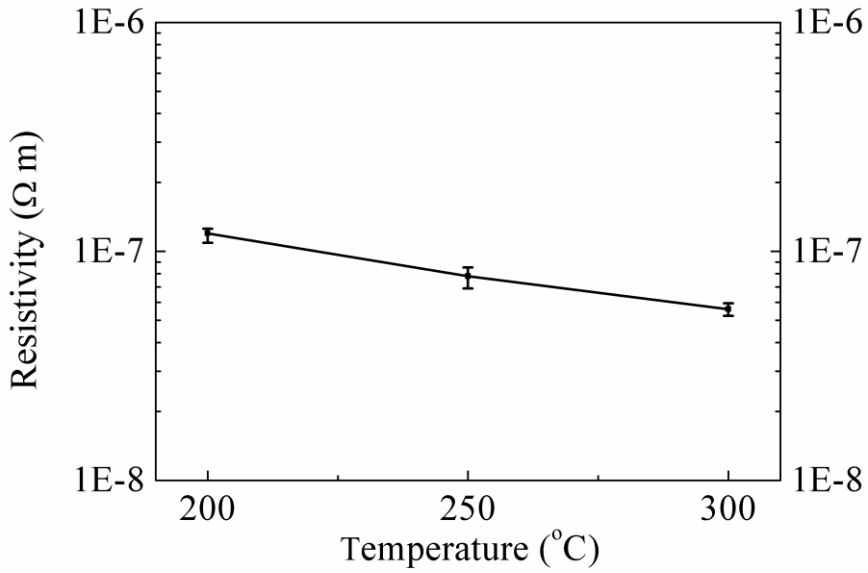

Fig. 2.13 Resistivity as a function of the two-step annealing temperature of copper A films after a two-step annealing process.

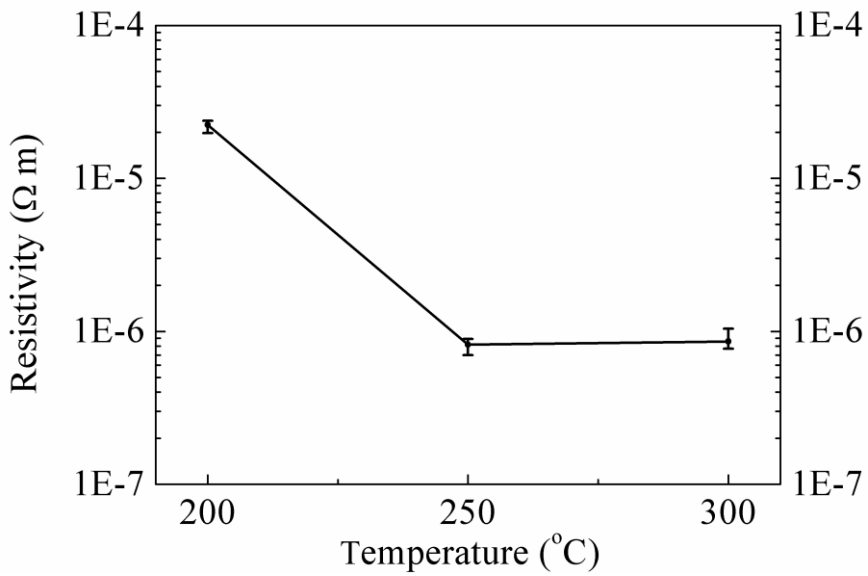

Fig. 2.14 Resistivity as a function of the two-step annealing temperature of copper B films after a two-step annealing process.

It is well understood that the particle sintering occurs when the organic capping layers on the surfaces of copper particles are removed and the necks between copper particles start to form.[20] At present, most of the studies carry out the sintering process directly without using the thermal oxidative preheating process to remove the organic capping layers [21,22] However, it should be noted that the oxidative preheating process can only remove the organic capping layers, but also can establish close contact between particles and form highly dense films with assistance of convex surfaces, oxide nanorods or oxide nanoparticles. And what is more, our approach in this study has two advantages. For the first advantage, our synthetic method of preparing copper fine particles avoids or mitigates the issues caused by using copper nanoparticles. Copper fine particles can be stored much easier compared with copper nanoparticles due to less oxidation under an ambient atmosphere. In addition, the synthesis of

copper fine particle does not need to utilize strong reducing agent. For the second advantage, in contrast with the approach of controlling particle size and preparing copper/silver core-shell nanoparticles[23] complicatedly and precisely, our thermal oxidation process which can also result in low resistivity at low sintering temperature is much more easy to handle.

2.4 Conclusions

In brief, a novel approach towards enhancing the electrical conductivity of obtained copper film has been developed. This approach which introduces a two-step annealing process can effectively result in formation of tight contacts between particles by producing convex surfaces, oxide nanorods or oxide nanoparticles. In the first step, copper fine particles were prepared by utilizing D-isoascorbic acid and octylamine as the mild reductant and the capping agent, respectively. In the second step, a thermal oxidative preheating process performed in air was introduced to produce convex surfaces, nanorods or nanoparticles. Produced convex surfaces, nanorods or nanoparticles during the thermal oxidative preheating process are caused by the diffusion of oxygen as well as diffusion of copper ion from the copper matrix to the surface. Owing to the critical role of the thermal oxidative preheating process which enhances particle sintering during the following reductive sintering process, copper films with low resistivities were obtained. We except that, our facile route for achieving low resistivity at low sintering temperature, which overcomes some problems caused by using copper nanoparticles, could open new possibilities for

printed electronics.

2.5 References

1 Li, A.; Song, H.; Zhou, J.; Chen, X.; Liu, S. CuO Nanowire Growth on Cu2O by In Situ Thermal Oxidation in Air. *CrystEngComm* **2013**, *15*, 8559-8564.

2 Filipič, G.; Cvelbar, U. Copper Oxide Nanowires: A Review of Growth. *Nanotechnology* **2012**, *23*, 194001.

3 Liu, Y. L.; Liao, L.; Li, J. C.; Pan, C. X. From Copper Nanocrystalline to CuO Nanoneedle Array. Synthesis, Growth Mechanism, and Properties. *J. Phys. Chem. C* **2007**, *111*, 5050-5056.

4 Li, X. Z.; Zhang, J.; Yuan, Y. W.; Liao, L. M.; Pan, C. X. Effect of Electric Field on CuO Nanoneedle Growth during Thermal Oxidation and Its Growth Mechanism. *J. Appl. Phys.*, *2010*, **108**, 024308.

5 Deng, S.; Tjoa, V.; Fan, H. M.; Tan, H. R.; Sayle, D. C.; Olivo, M.; Mhaisalkar, S.; Wei, J.; Sow, C. H. Reduced Graphene Oxide Conjugated Cu_2O Nanowire Mesocrystals for High-Performance NO_2 Gas Sensor. *J. Am. Chem. Soc.* **2012**, *134*, 4905-4917.

6 Zhang, Q.; Wang, H.-Y.; Jia, X.; Liu, B.; Yang, Y. One-Dimensional Metal Oxide Nanostructures for Heterogeneous Catalysis. *Nanoscale* **2013**, *5*, 7175-7183.

7 Ida, K.; Tomonari, M.; Sugiyama, Y.; Chujyo, Y.; Tokunaga, T.; Yonezawa, T.; Kuroda, K.; Sasaki, K. Behavior of Cu Nanoparticles Ink under Reductive Calcination for Fabrication of Cu Conductive Film. *Thin Solid Films* **2012**, *520*, 2789-2793.

8 Yabuki, A.; Arriffin, N. Electrical Conductivity of Copper Nanoparticle Thin Films Annealed at Low Temperature. *Thin solid films* **2010**, *518*, 7033-7037.

9 Narushima, T.; Tsukamoto, H.; Yonezawa, T. High Temperature Oxidation Event of Gelatin Nanoskin-Coated Copper Fine Particles Observed by In Situ TEM. *AIP Adv.* **2012**, *2*, 042113.

10 Xu, Z.; Shen, C.; Hou, Y.; Gao, H.; Sun, S. Oleylamine as Both Reducing Agent and Stabilizer in a Facile Synthesis of Magnetite Nanoparticles. *Chem. Mater.* **2009**, *21*, 1778-1780.

11 Huaman, J. L. C.; Sato, K.; Kurita, S.; Matsumotoc, T.; Jeyadevan, B. Copper Nanoparticles Synthesized by Hydroxyl Ion Assisted Alcohol Reduction for Conducting Ink. *J. Mater. Chem.* **2011**, *21*, 7062-7069.

12 Pulkkinen, P.; Shan, J.; Leppanen, K.; Kansakoski, A.; Laiho, A.; Jarn, M.; Tenhu, H. Poly(ethylene imine) and Tetraethylenepentamine as Protecting Agents for Metallic Copper Nanoparticles. *ACS Appl. Mater. Interfaces* **2009**, *1*, 519-525.

13 Guan, R.; Hashimoto, H.; Kuo, K. H. Electron-Microscopic Study of the Structure of Metastable Oxides Formed in the Initial Stage of Copper Oxidation. II. Cu_8O. *Acta Crystallogr., Sect. B: Struct. Sci.* **1984**, *40*, 560-566.

14 Guan, R.; Hashimoto, H.; Kuo, K. H. Kuo, Electron-Microscopic Study of the Structure of Metastable Oxides Formed in the Initial Stage of Copper Oxidation. III. $Cu_{64}O$. *Acta Crystallogr., Sect. B: Struct. Sci.* **1985**, *41*, 219-225.

15 Goncalves, A. M. B.; Campos, L. C.; Ferlauto, A. S.; Lacerda, R. G. On the Growth and Electrical Characterization of CuO Nanowires by Thermal Oxidation. *J. Appl. Phys.* **2009**, *106*, 034303.

16 Han, Z.; Lu, L.; Zhang, H. W.; Yang, Z. Q.; Wang, F. H.; Lu, K. Comparison of the Oxidation Behavior of Nanocrystalline and Coarse-Grain Copper. *Oxid. Met.* **2005**, *63*, 261-275.

17 Yabuki, A.; Tanaka, S. Oxidation Behavior of Copper Nanoparticles at Low Temperature. *Mater. Res. Bull.* **2011**, *46*, 2323-2327.

18 Wu, Y.; Yang, P. Direct Observation of Vapor-Liquid-Solid Nanowire Growth. *J. Am. Chem. Soc.* **2001**, *123*, 3165-3166.

19 Liu, C.; Hu, Z.; Wu, Q.; Wang, X. Z.; Chen, Y.; Sang, H.; Zhu, J. M.; Deng, S. Z.; Xu, N. S. Vapor-Solid Growth and Characterization of Aluminum Nitride Nanocones. *J. Am. Chem. Soc.* **2005**, *127*, 1318-1322.

20 Yang, C.; Wong, C. P.; Yuen, M. M. F. Printed Electrically Conductive Composites: Conductive Filler Designs and Surface Engineering. *J. Mater. Chem. C* **2013**, *1*, 4052-4069.

21 Deng, D.; Cheng, Y.; Jin, Y.; Qi, T.; Xiao, F. Antioxidative Effect of Lactic Acid-Stabilized Copper Nanoparticles Prepared in Aqueous Solution. *J. Mater. Chem.* **2012**, *22*, 23989-23995.

22 Jeong, S.; Lee, S. H.; Jo, Y.; Lee, S. S.; Seo, Y.-H.; Ahn, B. W.; Kim, G.; Jang, G.-E.; Park, J.-U.; Ryu, B.-H.; Choi, Y. Air-Stable, Surface-Oxide Free Cu Nanoparticles for Highly Conductive Cu Ink and Their Application to Printed Graphene Transistors. *J. Mater. Chem. C* **2013**, *1*, 2704-2710.

23 Grouchko, M.; Kamyshny, A.; Magdassi, S. Formation of Air-Stable Copper-Silver Core-Shell Nanoparticles for Ink-Jet Printing. *J. Mater. Chem.* **2009**, *19*, 3057-3062.

3. Systematic Study of Copper-Based Metal-Organic Decomposition Inks Using the Mixture of Copper Complex and Added Copper Particles for Low Temperature Sintering

3.1 Introduction

In general, two types of copper inks are frequently used.[1] One type of the copper inks is a suspension of copper particles including fine particles or nanoparticles. The other type is called copper-based metal-organic decomposition (MOD) ink. The MOD ink usually consists of copper salt, amino hydroxyl/amine ligands and other organic components. Copper-based MOD ink has been investigated widely for improving the electrical conductivity of obtained copper films at low sintering temperature due to its merits of scalability and simplicity. The purpose of adding the organic components (diethylene n-butanol,[2] glycol methyl ether,[2] 1-methyl-2-pyrrolidinone,[3] and ethyl cellulose,[3] octylamine,[4] etc.) in MOD ink is to improve the uniformity of the prepared copper inks and increase the electrical conductivity and reliability of obtained sintered copper films. But these organic additives are usually not conductor and make against decreasing the resistivity of copper films after sintering by inhibit the contact between copper fine particles or nanoparticles.

In this study, we put forward a new route to improve the uniformity of the copper inks and the conductivity of copper films at low sintering temperature. This new route can overcome the above mentioned obstacle by replacing the organic components by

commercial copper fine particles. The choice of copper sources, i.e. copper acetate (CuA) and copper formate (CuF), in the formation of copper complexes as the copper were compared. Added commercial particle size on the conductivity of copper films after sintering was studied. Furthermore, polyvinylpyrrolidone (PVP) capped copper particles with smaller size were also prepared as the added particles for the preparation of copper-based MOD inks. The use of PVP capped copper particles as the added copper particles can prove the general applicability of our proposed method in this work.

3.2 Experimental section

3.2.1 Formation of commercial copper fine particle/copper acetate-IPA (1-amino-2-propanol)-ethanol (EOH) mixed inks (Cu/CuA-IPA-EOH) and sintered conductive copper films

Copper (II) acetate monohydrate ($Cu(CO_2CH_3)_2 \cdot H_2O$, CuA) (Kanto, Japan) was chosen as a copper source for the formation of copper ink. Isopropanolamine (1-amino-2-propanol, IPA) (Junsei, Japan, GR grade) was chosen as the ligand. After mixing CuA (2.5 mmol, 0.5 g), IPA (5 mmol, 0.375g) and ethanol (Kanto, 5 mmol, 0.23 g, EOH) using conditioning mixer, 50 wt% commercial copper fine particles (DOWA, 0.5μm, as shown in Fig. 3.1) were put into the mixture with another mixing for 16 min. After that, the obtained inks were printed onto alumina substrates with a doctor blade (the thickness of printed films were 40 μm) and sintered at different temperatures (120 ℃ and 150 ℃) with a N_2 flow for various periods.

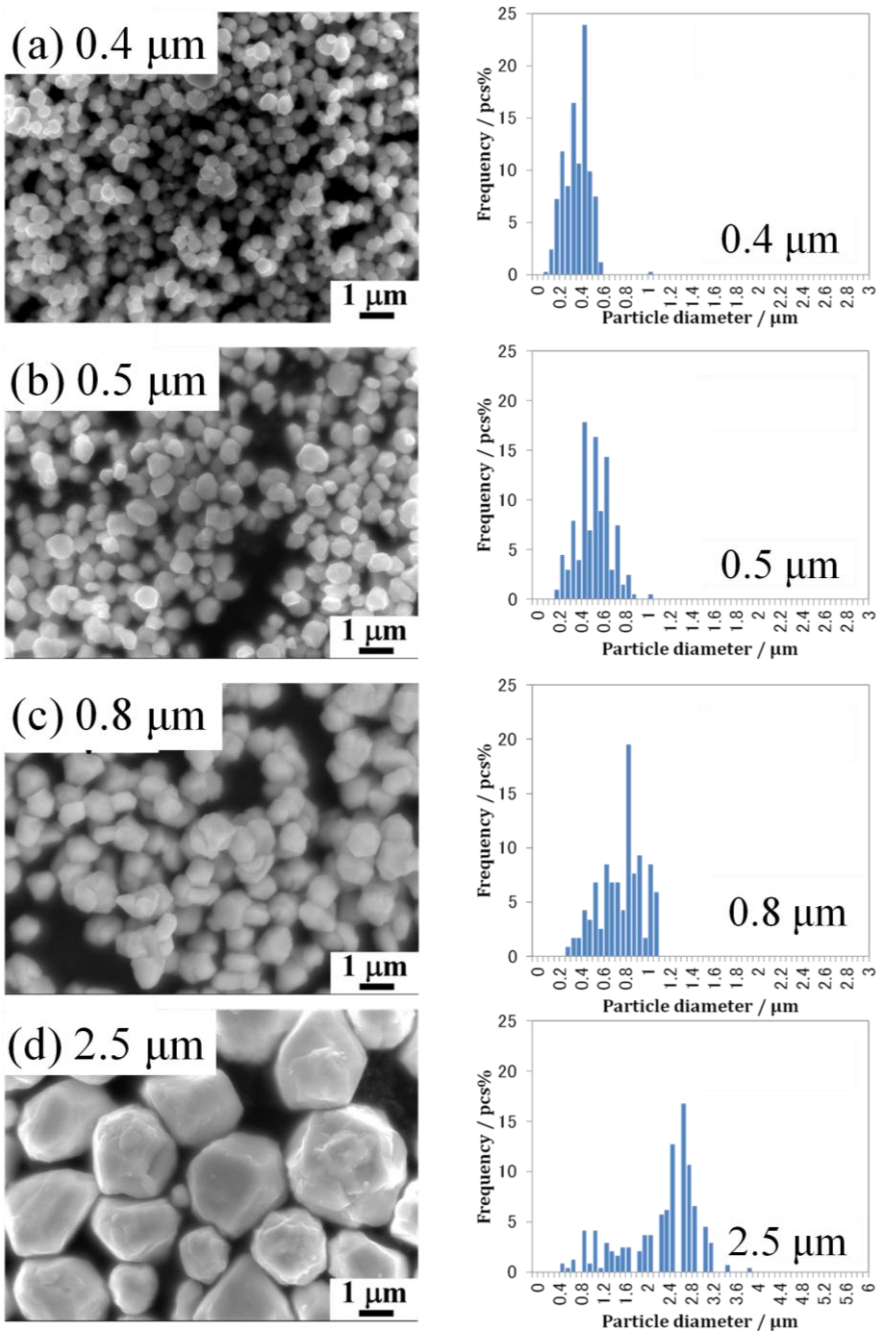

Fig. 3.1 SEM images and size distributions of added commercial copper fine particles. The average sizes of added copper particles were (a) 0.4 μm, (b) 0.5 μm, (c) 0.8 μm and (d) 2.5 μm. The copper fine particles with size of 0.8 μm comes from our previous work.[5]

3.2.2 Formation of commercial copper fine particles/copper formate-IPA mixed inks (Cu/CuF-IPA) and sintered conductive copper films

Besides CuA, copper (II) formate tetrahydrate ($Cu(HCOO)_2 \cdot 4H_2O$, CuF) (Wako,

Japan) was also selected as the other copper source. Similar to the procedure of preparation of Cu/CuA-IPA-EOH inks, CuF (5 mmol, 1.13 g), IPA (10 mmol, 0.75) commercial copper fine particles (Dowa, Japan) with a median size of 0.4, 0.5, 0.8, and 2.5 μm were mixed by conditioning mixer. The weight amount of added commercial copper fine particles was 50 wt%. For comparison, 70 wt% of commercial copper fine particles with the size of 0.4 μm were also put into CuF-IPA complex. The prepared inks were also printed on alumina substrates by using a doctor blade (40 μm) and dried under a N_2 flow at 60 ℃ for 1 h. Finally, the printed inks were heated under a N_2 gas at 120 ℃ for various periods (30 min or 1 h).

3.2.3 Synthesis of copper/polyvinylpyrrolidone particles (PVP-Cu)

Firstly, 1.2 g polyvinylpyrrolidone (PVP, MW=10000, Tokyo Chemical Industry Co., Japan) was dissolved in 60 cm^3 1,5 pentanediol (98%, Junsei Chemical Co., Japan). Then 1.2 g CuO was added into above solution. After that, the mixture was heated in an oil bath to 80 ℃. Hydrazine monohydrate (Junsei) as the reducing agent was added into the above mixture dropwise. This chemical reaction was kept for 4 h. After centrifugation with 1-propanol and drying under a N_2 flow, PVP-Cu particles were obtained.

3.2.4 Fabrication of PVP-Cu/CuF-IPA mixed inks and their sintered copper films

CuF (1 mmol, 0.23 g) and IPA (2 mmol, 0.15 g) were well mixed using a conditioning mixer. PVP-Cu particles were added into prepared CuF-IPA complex and mixed with a conditioning mixer for 12 min. The weight percent of added PVP-Cu in the ink was

50 wt%. Following mixing, the prepared inks were printed and heated using the same way as Cu/CuF-IPA inks. The heating temperature was 100 ℃ under a N_2 gas. In addition, the ink with another ratio with the same process was also prepared. The ratio between CuF (4 mmol, 0.90 g) and IPA (4 mmol, 0.30 g) was 1:1 (mol/mol). The weight percent of PVP-Cu particles (0.51 g) was 30 wt%. Then the ink was also sintering at 100 ℃ under a N_2 gas.

3.2.5 Characterization

Scanning electron microscopy (SEM) images of the added commercial copper particles, PVP-Cu particles and Cu films, thicknesses of the sintered copper films used for calculating the bulk resistivities of sintered copper films were got by using a JEOL JSM-6701F field-emission-type SEM. X-ray diffraction (XRD) patterns were obtained by using a Rigaku Miniflex-II diffractometer. Thermogravimetric differential thermal analysis (TGA-DTA) was carried out by using a Shimadzu DTG-60H to study the decomposition process of the mixture of CuA-IPA complex and ethanol. The sheet resistances of copper films were measured with a four-point probe by using a Mitsubishi Chemical Analytech Loresta-GP with an ASP probe.

3.3 Results and discussion

3.3.1 The choice of copper source

Copper formate (CuF) as one kind of copper source used for the fabrication of copper-based MOD inks has been extensively studied[2-7]. CuF as the copper source has

the following advantages: (i) the produced products (i.e., H_2 and CO_2) during the decomposition are volatile and no undesired residues which may decrease the conductivity of copper films remain in the obtained conductive copper films. Furthermore, the generated H_2 gas is conducive to maintaining a reducing atmosphere which can prevent the particle oxidation. (ii) there is high copper content due to the short carbon chain in the CuF. (iii) the low decomposition temperature allow to use the temperature sensitive but low-cost substrates for printed electronics.[2]

However, formic acid is corrosive. In comparison, acetic acid is more preferred for preventing the furnace failures. Copper acetate (CuA) is also regarded as another choice as the copper source. The advantages of CuA are as following: (i) it is easy to be prepared. The production of CuA on a large scale for commercial use utilizes copper metal in air and refluxing acetic acid.[8] (i) there is also high copper content in CuA. (ii) it has low decomposition temperature. (iii) the decomposition of CuA can also generate volatile H_2 which can help keep a reducing atmosphere (eq. 2). (iv) CuA has good solubility in alcohol solvents. Due to alcohol solvents are friendly for blanket layer in the reverse offset printing which is used for large-scale production with high resolution, alcohol-solvent-based conductive inks are preferred for the commercial printing.[4] Esqs. 1-2 as following exhibits the decomposition of CuA. [9,10]

$$Cu(CO_2CH_3)_2 \cdot H_2O \rightarrow Cu(CO_2CH_3)_2 + H_2O \quad (1)$$

$$Cu(CO_2CH_3)_2 \rightarrow Cu + 3H_2 + CO_2 + C \quad (2)$$

In this study, we firstly compared the two kinds of copper sources (i.e., CuA and CuF) to prepare the mixture with IPA as well as commercial copper fine particles with a size of 0.5 μm. Based on our previous study, CuF can have decomposition at the temperature as low as ~100 ℃ with the assist of IPA.[5] The decomposition of CuA and IPA were investigated by the TG/DTA measurement as shown in Fig. 3.2. There are two stages primarily during the decomposition of mixture of CuA, IPA and EtOH. Before 121 ℃, there were ~30 wt% losses including 20 wt% of EtOH evaporation , 9 wt% water from the dehydration of CuA (eq. 1) and small amount of IPA. The decomposition process of CuA commenced from ~120 ℃ and totally finished at ~300 ℃.

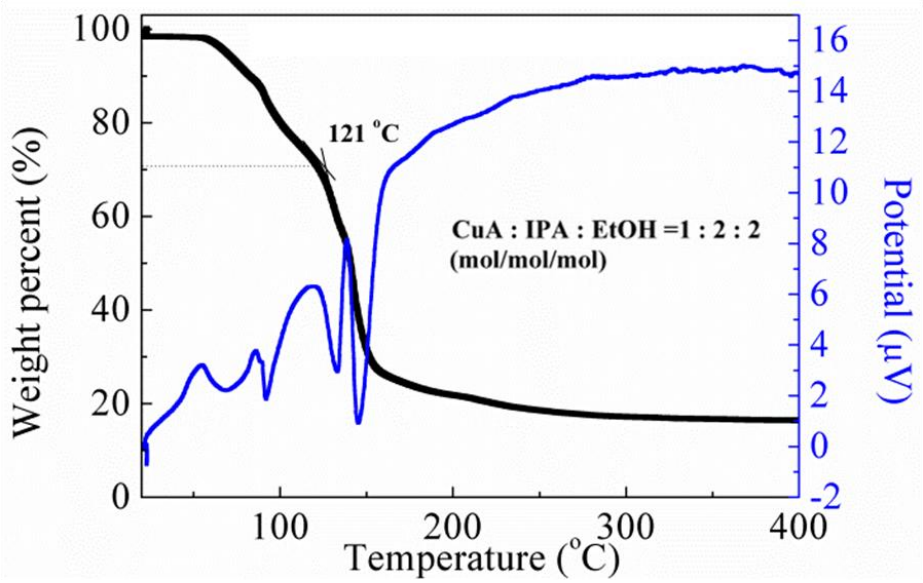

Fig. 3.2 TG/DTA curves of CuA-IPA-EtOH mixture (CuA : IPA : EOH =1:2:1, mol/mol/mol) under a N_2 flow. The mixture was kept under a N_2 flow in the measurement equipment for 150 min to exchange gas from air to N_2. The heating condition is from room temperature to 800 ℃ with a heating rate of 2.3 ℃/min. The evaporation of small amount of water and EtOH at room temperature was caused by gas exchange.

According to the above TG measurement, the sintering temperature of the fabricated Cu/CuA-IPA-EOH inks was decided to be 120 ℃. The XRD results of the inks printed and sintered under a N_2 flow at 120 ℃ for various time were exhibited in Fig. 3.3. After sintering process at 120 ℃ for 30 min and 2 h, an impurity peak at ~10 degree were detected from these sintered films. In comparison with the XRD pattern of printed films, it can be deduced that this impurity peak is from the ink which did not decompose totally after heating for 30 min and 2 h. Hence, higher sintering temperature was tried. Fig. 3.4 shows the XRD patterns of the inks after sintering at 150 ℃ for 30 min and 1 h. Following sintering for 30 min and 1 h, the impurity peak at ~10 degree disappeared (Fig. 3.4). Metallic copper peaks without any the impurity peak at ~10 degree were found in the copper films after sintering at 150 ℃ (Fig. 3.4). Fig. 3.5 shows the reliability of sintered copper films using Cu/CuA-IPA-EOH inks. There is negligible change about the sheet resistances of copper films following sintering for 30 min and 1 h within 5 days.

To decide which copper source should be used, the resistivities of copper films obtained using Cu/CuF-IPA and Cu/CuA-IPA-EtOH inks were compared. Fig. 3.6 shows the resistivities of copper films for various temperatures after sintering by using Cu/CuF-IPA and Cu/CuA-IPA-EtOH inks. For Cu/CuA-IPA-EtOH inks, after sintering at 150 ℃ for 30 min and 1 h under a N_2 flow, the obtained resistivities of copper films were 5.9×10^{-6} and 3.7×10^{-6} Ω m, respectively. For the Cu/CuF-IPA inks, the copper film following sintering 120 ℃ for 30 min can achieve the resistivity of 3.2×10^{-7} Ω m.

Based on the above results, CuF was selected as the copper source for the other studies in this work.

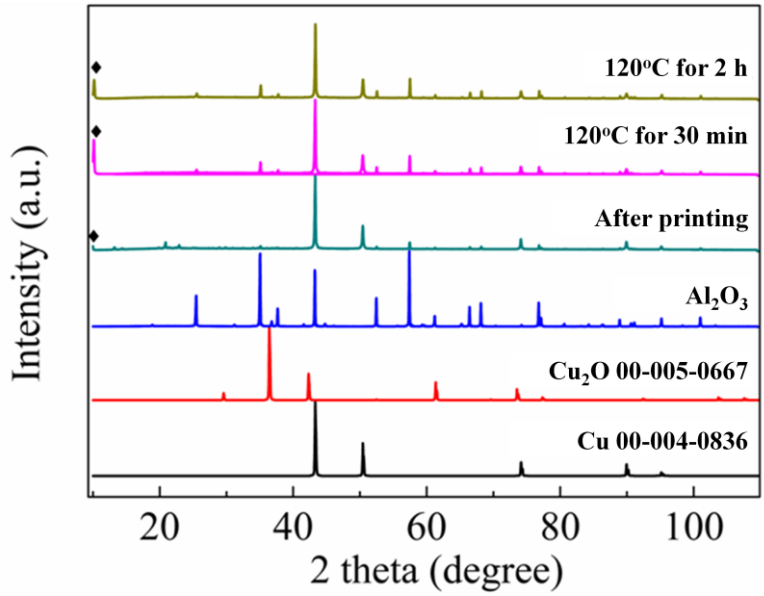

Fig. 3.3 XRD of the sintered copper films using Cu/CuA-IPA-EOH inks after printing and sintering under a N_2 flow at 120 ℃ for various periods.

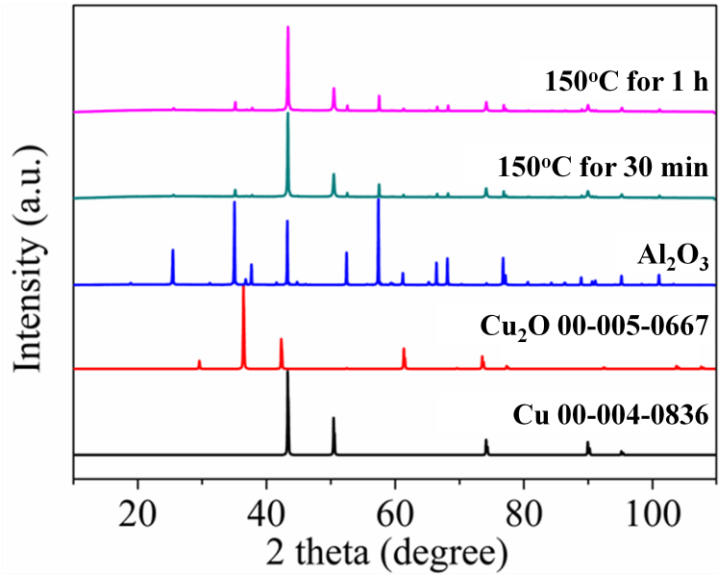

Fig. 3.4 XRD of the sintered copper films using Cu/CuA-IPA-EOH inks after sintering under a N_2 flow at 150 ℃ for various periods.

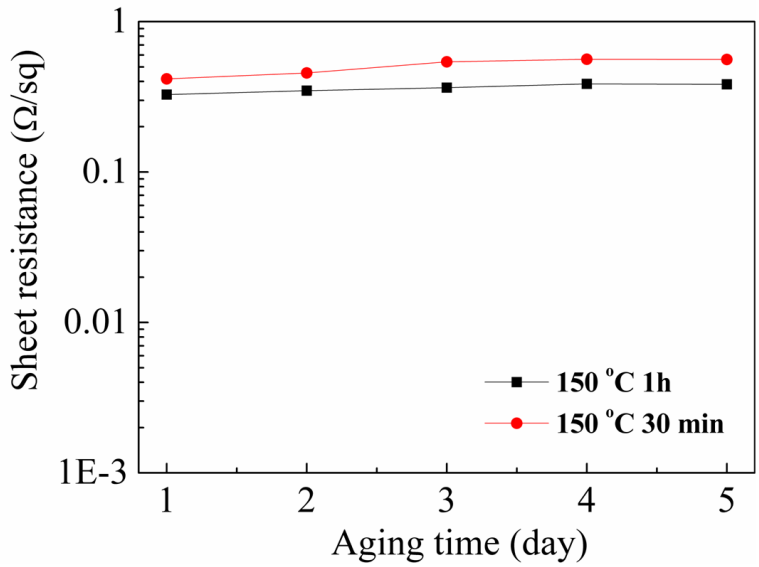

Fig. 3.5 Corresponding sheet resistance shifts of copper films using Cu/CuA-IPA-EOH inks sintered at 150 ℃ at various time with time aging at room temperature in air.

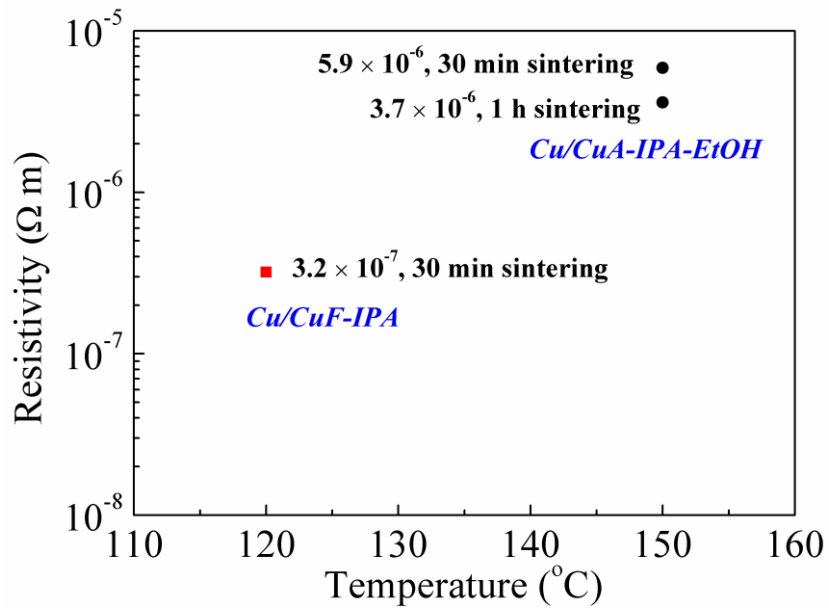

Fig. 3.6 Resistivities of obtained copper films using Cu/CuF-IPA and Cu/CuA-IPA-EtOH inks after sintering process at various temperatures.

3.3.2 The effect of the size of added copper particle size on the obtained resistivity of copper film after sintering process

After deciding the copper source based on the above results, the influence of the size of added copper particles on the resistivity of obtained copper films were studied. The sizes of used copper fine particles were 0.4, 0.5, 0.8 and 2.5 μm. Fig. 3.7 presents the resistivities of the copper films using Cu/CuF-IPA inks (CuF : IPA = 1 : 2 (mol/mol) inks following sintering at 120 ℃ for 30 min under a N_2 gas. The obtained conductive copper films which were prepared with 0.4, 0.5, 0.8 and 2.5 μm of the added copper particles presents low resistivity of 2.6×10^{-7}, 3.2×10^{-7}, 1.1×10^{-6}, and 1.9×10^{-6} Ω m, respectively. From the SEM images of added copper particle shown in Fig. 3.1, it can be deduced that the melting of such micron particles at such a low temperature is impossible due to the well-known Gibbs-Thomson equation which demonstrates the relationship between the melting point and the particle size. Hence, the low resistivities of obtained conductive copper films are due to the close contact among particles. From Fig. 3.7, it can be found that the resistivity of obtained copper film decreases with the decrease of the size of the added commercial copper particles. This can be ascribed to that less vacancy is remained by using smaller added copper particles. CuF can generate copper atoms by decomposition to deposit in the vacancy between the added copper particles, which can be confirmed by the SEM images of the sintered conductive copper films as shown in Fig. 3.8. More connections between copper particles could be observed when smaller added copper particles were chosen, thus leading to lower resistivity. From Fig. 3.7, it can be also found that the

relationship between the resistivity and size of added copper particles presents linear relation when the size of added copper particles was less than a certain size (0.8 μm); when the size of added copper particles was more than this size, a nonlinear curve with a flat appeared. These results are because that the resistivity of sintered copper films is strongly related to the spaces between particles which can be filled in by deposited copper atoms from CuF. However, if the size of added copper particle was more than a certain size, the vacancy among particles has no big difference even using added copper particles with larger size (Figs. 5c and 5d). Hence, the resistivity had a tendency to be stable.

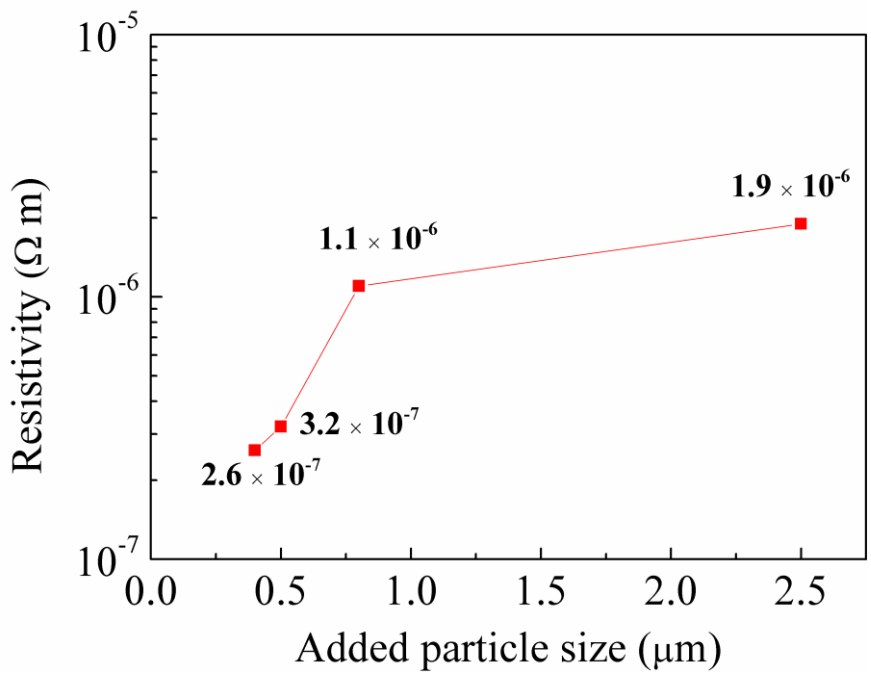

Fig. 3.7 Resistivities of the obtained copper films using Cu/CuF-IPA inks (CuF : IPA = 1 : 2 (mol/mol) inks after sintering at 120 ℃ for 30 min under a N_2 gas. The sizes of added commercial copper particles were 0.4, 0.5, 0.8, and 2.5 μm, respectively.

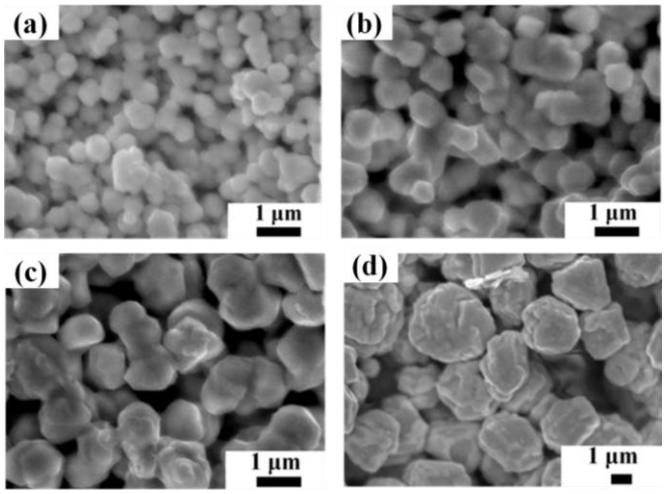

Fig. 3.8 Morphological images of the conductive copper films following sintering at 120 ℃ by using the Cu/CuF-IPA inks with added copper particles with various sizes: (a) 0.4, (b) 0.5, (c) 0.8, and (d) 2.5 μm. In the prepared ink, the molar ratio of CuF to IPA was 1 to 2 and the weight amount of added copper particles was 50 wt%.

3.3.3 The amount of added copper particles and optimal sintering time

In this study, the amount of added copper particles as well as the optimal sintering time was also investigated by using the added copper particles with size of 0.4 μm for the preparation of inks.

50 wt% and 70 wt% of added copper particles were put into the prepared CuF-IPA complex, respectively. By comparison, the obtained ink with 70 wt% of added copper particles has very high viscosity which is not suitable for well printing. Hence, the optimal amount of added copper particles for the preparation of ink was 50 wt%.

Table 3.1 presents the sheet resistances of obtained copper films following sintering at 120 ℃ under a N_2 flow for 30 min and 1 h. There is no obvious difference for the sheet resistance between films after sintering for 30 min and 1 h. 30 min was

suitable for the sintering process.

Table 3.1. Sheet resistances of the obtained conductive copper films using Cu/CuF-IPA inks after sintering under a N_2 flow at 120 ℃ for various periods (CuF : IPA = 1 : 2 (mol/mol))

Sintering time (h)	0.5	1
Sheet resistance (Ω/sq)	4.2×10^{-2}	5.7×10^{-2}

3.3.4 The influence of the organic residual on the resistivity of obtained conductive copper film

Based on the above analyses, it was found that less vacancy in the sintered copper films can be obtained using smaller particles as the added cooper particle. Hence, PVP capped copper particles with smaller particles size were prepared to replace the added commercial copper fine particles for lower temperature sintering (100 ℃).

Fig. 3.9 shows the SEM image, XRD, size distribution and TG of the prepared PVP-Cu particles. XRD pattern in Fig. 3.9b shows a minor peak corresponding to Cu_2O besides metallic copper peaks. The size of prepared PVP-Cu particles is 127 ± 20 nm (Fig. 3.9c). From the TG result of PVP-Cu particles (Fig. 3.9d), the organic weight amount in PVP-Cu particles was 3 wt% which can be calculated from the final generated CuO after oxidation in air. Fig. 3.10 is the XRD pattern of conductive copper films following sintering under a N_2 flow at 100 ℃ for 1 and 2 h by using PVP-Cu/CuF-IPA inks. No oxides were found, which are due to IPA and produced

hydrogen during the decomposition of CuF-IPA complex. IPA can reduce copper oxide to metallic copper and hydrogen can keep a reducing atmosphere to prevent oxidation.

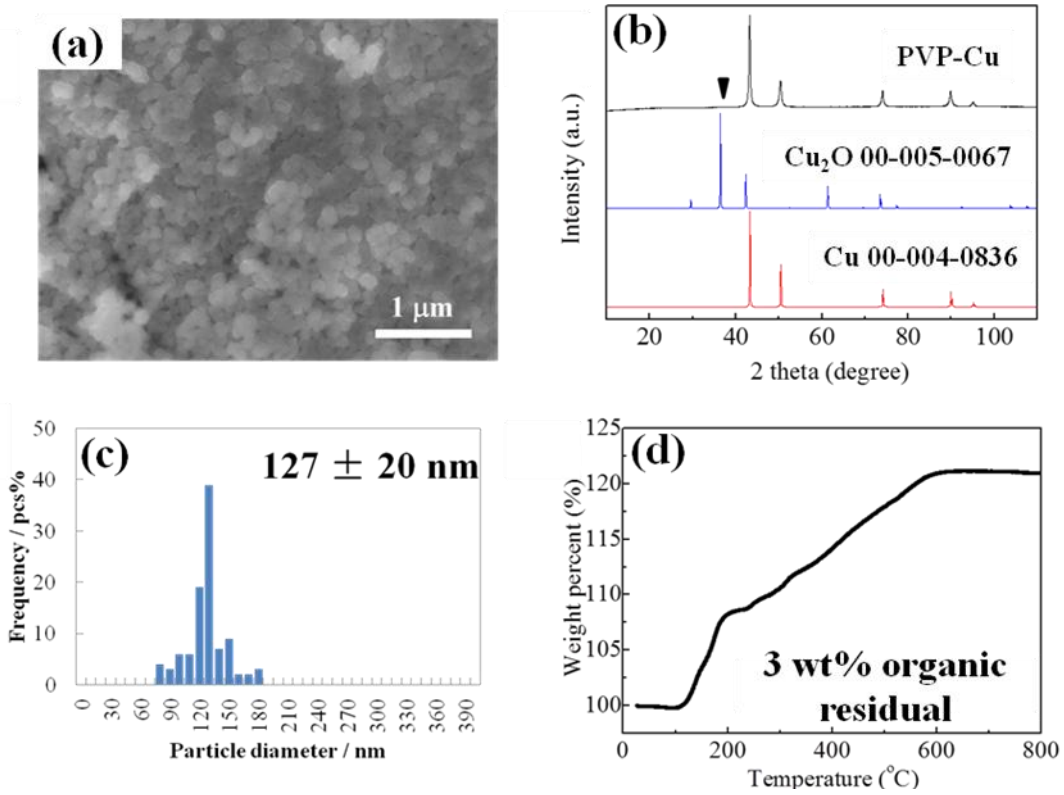

Fig. 3.9 Morphological image (a), XRD pattern (b), size distribution (c) and TG (d) of prepared PVP-Cu particles. The TG measurement was performed in air from room temperature to 800 ℃.

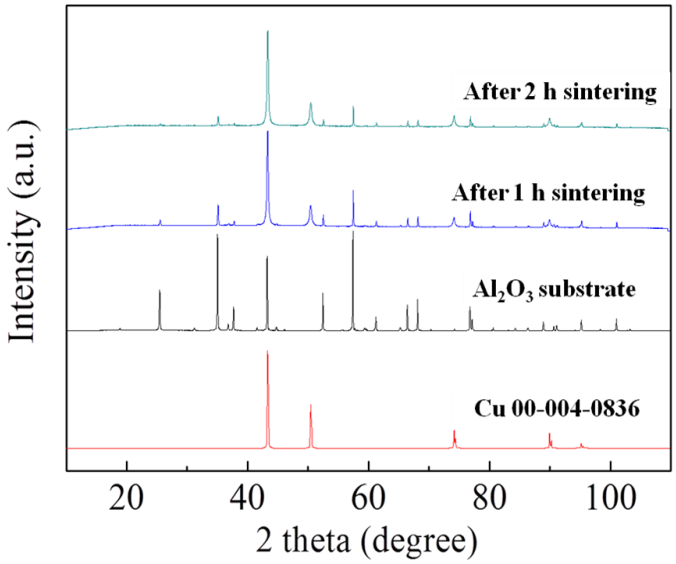

Fig. 3.10 XRD of copper films obtained from PVP-Cu/CuF-IPA inks (CuF : IPA = 1 : 2 (mol/mol), 50 wt% PVP-Cu) following sintering process under a N_2 flow at 100 ℃ for 1 and 2 h.

The morphological images of conductive copper films which were obtained using PVP-Cu/CuF-IPA inks following sintering process under a N_2 flow at 100 ℃ for 1 and 2 h were shown in Fig. 3.11. According to these SEM images, the copper films obtained using PVP-Cu particles which were smaller than commercial copper particles as the added particles present less vacancy. This is in accordance with the above results and our assumption. But it was found that these copper films after sintering did not present lower resistivities.

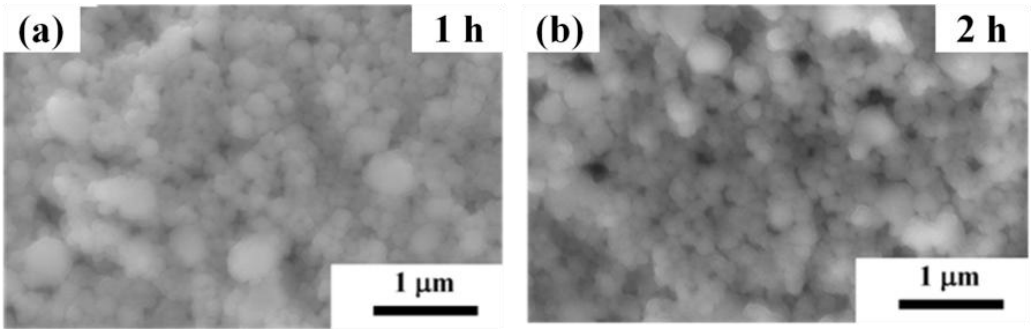

Fig. 3.11 Morphological images of copper films obtained using PVP-Cu/CuF-IPA inks after sintering at 100 ℃ for 1 and 2 h. (CuF : IPA = 1 : 2 (mol/mol), 50 wt% Cu).

The resistivities of conductive copper films following sintering process under a N_2 flow at 100 ℃ for 1 and 2 h by using PVP-Cu/CuF-IPA inks are shown in Table 3.2. The resistivities of conductive copper film after 1 h and 2 h sintering were over range and 1×10^{-4} Ω m, respectively. In contrast, the conductive copper film which used 0.4 μm of commercial copper fine particles as added copper particles after sintering at 100 ℃ for 1 h could have some conductivity (4.3×10^{-2} Ω/sq of the sheet resistance).

Table 3.2. Resistivities of the conductive copper films obtained using PVP-Cu/CuF-IPA inks after sintering process under a N_2 flow at 100 ℃. (CuF : IPA = 1 : 2, 50 wt% PVP-Cu or CuF : IPA = 1 : 1 (mol/mol), 30 wt% PVP-Cu).

Sintering time at 100 ℃	Resistivity (Ω m)	
	CuF:IPA = 1 : 2 with 50 wt% PVP-Cu	CuF:IPA = 1 : 1 with 30 wt% PVP-Cu
1 h	Over range	19.4
2 h	1×10^{-4}	7×10^{-6}

To investigate the possible reasons, the amount of organic residual was performed using TG measurements. After sintering process under a N_2 gas flow at 100 ℃ for 1 h, copper films using Cu (0.4 μmϕ)/CuF-IPA inks and PVP-Cu/CuF-IPA inks have the 2 wt% and 5 wt% of organic residual, respectively. In combination with the morphological images shown in Figs. 3.8a and 3.11a, it could be found that the high resistivity of copper film obtained using PVP-Cu/CuF-IPA ink and following sintering for 1 h at 100 ℃ was due to much organic residual. Furthermore, the amount of organic residual in the conductive copper film following sintering at 100 ℃ decreased from 5 wt% to 4 wt% when the sintering time increased from 1 h to 2 h. Hence, the weight amount of PVP-Cu and IPA in the inks was reduced to further reduce the resistivity of the sintered conductive copper film. The IPA amount was reduced (the mole ratio of CuF to IPA decreased from 1:2 and 1:1). In addition, the PVP amount was reduced by decreasing the amount of the added PVP-Cu particles from 50 wt% to 30 wt%. After sintering process under a N_2 flow at 100 ℃ for 2 h, the copper film (Fig. 3.13) without oxides can have the resistivity of 7×10^{-6} Ω m (Table 3.2).

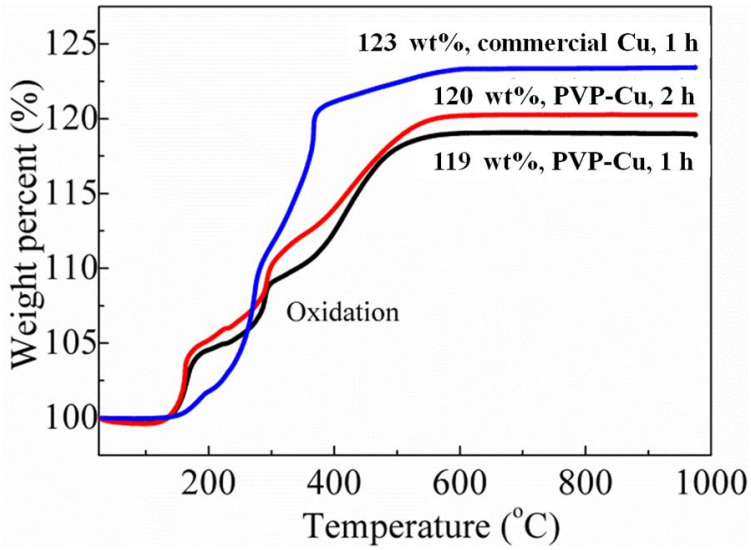

Fig. 3.12 TG curves of conductive copper films following sintering at 100 ℃ by using Cu (0.4 μmϕ, commercial particles)/CuF-IPA inks for 1 h (CuF : IPA = 1 : 2 (mol/mol), 50 wt% Cu) (blue) and PVP-Cu/CuF-IPA inks for 1 h (black) and 2 h (red).

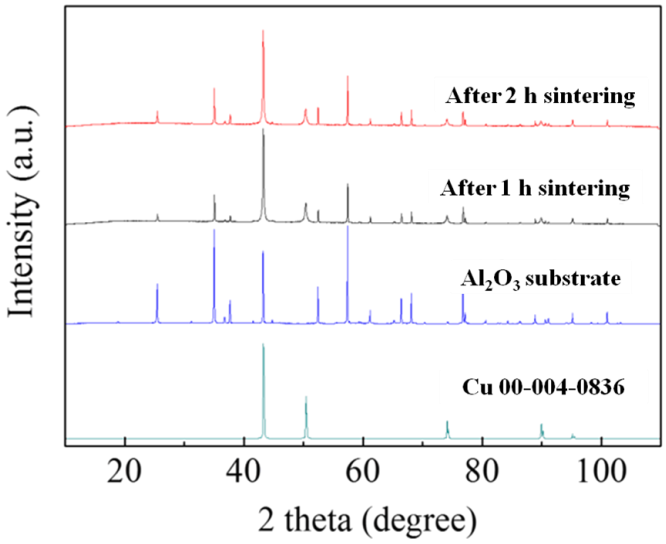

Fig. 3.13 XRD of conductive copper films got by using PVP-Cu/CuF-IPA inks after sintering process for 1 and 2 h at 100 ℃ (CuF : IPA = 1 : 1 (mol/mol), 30 wt% PVP-Cu).

According to the above analyses, it can be found that if the added copper particles

used the same capping agent, the resistivity of obtained copper film is strongly elated to the size of added copper particle. The resistivity decreases with the decrease of size of added copper fine particles. If the size of added copper fine particle is more than a certain size (0.8 μm), the space between the copper particles after the deposition of copper atoms has no obvious difference even the size of added copper fine particles was further increased. If the capping agents of the added copper particles are different, the amount of organic residual has a critical effect on the resistivity of obtained conductive copper film when the degree of space is similar. The above results exhibit that the approach of using the mixture of CuF-IPA complex and added copper particles for the fabrication of MOD inks has a general applicability for achieving low temperature sintering of copper films. Not only the commercial copper fine particles but also prepared PVP-Cu particles could be utilized as the added particles for the preparation of the inks. A low resistivity of 7×10^{-6} Ω m was achieved by sintering PVP-Cu/CuF-IPA inks at 100 ℃ under a N_2 flow.

3.4 Conclusions

In brief, the approach of using the mixture of copper-amino alcohol complex and added copper particles for the preparation of MOD inks to achieve low temperature sintering (≤150 ℃), was investigated systemically. It was demonstrated that CuF as the copper source for the preparation of copper-based MOD inks could lead to lower resistivity with lower temperature sintering in comparison with CuA. The copper film with a resistivity of 3.2×10^{-7} Ω m was obtained by choosing CuF as the copper

source and sintering at 120 ℃ for 30 min under a N_2 flow. The resistivity of sintered conductive copper films (using CuF as the copper source) decreased when the size of added copper particle decreased. The lowest resistivity (2.6×10^{-7} Ω m) was achieved following sintering at 120 ℃ under a N_2 flow by choosing 0.4 μm of added commercial copper particles. Furthermore, PVP-Cu particles (127 ± 20 nm) were prepared to replace the commercial copper particles for the preparation of copper-based MOD inks. The resistivity of the conductive copper film by using PVP-Cu particles as the added copper particles after sintering at 100 ℃ under a N_2 flow was 7×10^{-6} Ω m. The above results indicate that the approach of mixing copper complex with added copper particles are promising and has general applicability.

3.5 References

1 Perelaer, J.; Smith, P. J.; Mager, D.; Soltman, D.; Volkman, S. K.; Subramanian, V.; Korvink, J. G.; Schubert, U. S. Printed Electronics: The Challenges Involved in Printing Devices, Interconnects, and Contacts Based on Inorganic Materials. *J. Mater. Chem.* **2010**, *20*, 8446-8453.

2 Farraj, Y.; Grouchko, M.; Magdassi, S. Self-Reduction of a Copper Complex MOD Ink for Inkjet Printing Conductive Patterns on Plastics. *Chem. Commun.* **2015**, *51*, 1587-1590.

3 Choi, Y.-H.; Hong, S.-H. Effect of the Amine Concentration on Phase Evolution and Densification in Printed Films Using Cu (II) Complex Ink. *Langmuir* **2015**, *31*, 8101-8110.

4 Shin, D.-H.; Woo, S.; Yem, H.; Cha, M.; Cho, S.; Kang, M.; Jeong, S.; Kim, Y.; Kang, K.; Piao, Y. A Self-Reducible and Alcohol-Soluble Copper-Based Metal-Organic Decomposition Ink for Printed Electronics. *ACS Appl. Mater. Interfaces* **2014**, *6*, 3312-3319.

5 Yonezawa, T.; Tsukamoto, H.; Yong, Y.; Nguyen, M. T.; Matsubara, M. Low Temperature Sintering Process of Copper Fine Particles under Nitrogen Gas Flow with Cu 2+-Alkanolamine Metallacycle Compounds for Electrically Conductive Layer Formation. *RSC advances* **2016**, *6*, 12048-12052.

6 Yabuki, A.; Tanaka, S. Electrically Conductive Copper Film Prepared at Low Temperature by Thermal Decomposition of Copper Amine Complexes with Various Amines. *Mater. Res. Bull.* **2012**, *47*, 4107-4111.

7 Kim, S. J.; Lee, J.; Choi, Y.-H.; Yeon, D.-H.; Byun, Y. Effect of Copper Concentration in

Printable Copper Inks on Film Fabrication. *Thin Solid Films* **2012**, *520*, 2731-2734.

8 Richardson, H. W. *Handbook of Copper Compounds and Applications*; Marcel Dekker: New York, 1997.

9 Afzal, M.; Butt, P. K.; Ahrnad, H. Kinetics of Thermal Decomposition of Metal Acetates. *J. Therm. Anal.* **1991**, *37*, 1015-1023.

10 Obaid, A. Y.; Alyoubi, A. O.; Samarkandy, A. A.; Al-Thabaiti, S. A.; Al-Juaid, S. S.; El-Bellihi, A. A.; Deifallah, El-H. M. Kinetics of Thermal Decomposition of Copper (II) Acetate Monohydrate. *J. Therm. Anal. Calorim.* **2000**, *61*, 985-994.

11 Yang, C.; Wong, C. P.; Yuen, M. M. F. Printed Electrically Conductive Composites: Conductive Filler Designs and Surface Engineering. *J. Mater. Chem. C* **2013**, *1*, 4052-4069.

12 Deng, D.; Jin, Y.; Cheng, Y.; Qi, T.; Xiao, F. Copper Nanoparticles: Aqueous Phase Synthesis and Conductive Films Fabrication at Low Sintering Temperature. *ACS Appl. Mater. Interfaces* **2013**, *5*, 3839-3846.

4. Mixture of Decomposable Polymer-Coated Submicron Copper Particles and Effective Additive as the Ink for Obtaining Highly Conductive Copper Films following Low Temperature Sintering

4.1 Introduction

There are some researches which studied the surface modification of nanoparticles for achieving low temperature sintering of metal particles. Magadassi and co-workers have triggered silver nanoparticles sintering using desorption of the stabilizer from particle surfaces or charge neutralization.[1] Long et al. have developed an approach towards rapid sintering of silver nanoparticles through the ion pairs formation between the benzoquinone and cations from the electrolyte. The coalescence of silver nanoparticles occurred at room temperature due to the formation of the ion pairs which can break the balance state between the benzoquinone and silver atoms at the surface of particles.[2] Grouchko et al. have utilized a built-in sintering mechanism to facilitate particle sintering. This built-in sintering mechanism worked when the stabilizer detached from the surface of the particle by using a destabilizing agent. Room temperature coalescence of the silver particles took place.[3]

In our previous study, our group has proposed a novel method for achieving low temperature sintering of copper particles by using the ink prepared by mixing a copper complex and copper fine particles, and without any surface modification.[4] In

this work, in order to further decrease the resistivity of copper films following sintering at low temperature, decomposable polymer (polypropylene carbonate, PPC) capped copper particles with smaller size were utilized in the preparation of copper-based MOD inks, which were mixed with copper formate (CuF) and 1-amino-2-propanol (IPA) complex. PPC capped copper particles with a smaller size and a wider size distribution could have good effects on the stability of the inks, and also enhance the contacts between the copper particles to form denser copper film. In addition, the decomposable PPC as the ligand of the added copper particles were break down by an aminolysis with IPA, consequently triggering the particle coalescence and sintering. In this work, the synergistic effects due to the presence of CuF-IPA additive and decomposable polymer-stabilized copper particles on the low resistivity of copper film at low sintering temperature were demonstrated. A conductive copper film with a resistivity of 8.8×10^{-7} Ω m was produced by sintering under a N_2 gas flow at 100 ℃.

4.2 Experimental section

4.2.1 Synthesis of PPC-capped copper fine particles (PPC-Cu)

Firstly, 3.6 g PPC (Sumitomo Seika Chemicals Co., Japan) was dissolved in 180 cm^3 tetrahydrofuran (THF, Kanto). Then, 3.6 g cupric oxide (CuO) (Nissin Chemco, Japan), agglomerates with sizes in the range from a few hundred nanometers to several micrometers, was put into the above prepared solution, following being heated to 60 ℃ with a stirring speed of 433 rpm. After that, 10.8 cm^3 hydrazine monohydrate

(Junsei) was added into the mixture, accompanied with a color change from black to brown-red. The reaction was kept for 1 h. After centrifugation procedure for three times by using ethanol and ethyl acetate and drying under a N_2 gas, PPC-capped copper particles were prepared.

4.2.2 Fabrication of PPC-capped copper particles/$Cu(HCOO)_2$-IPA (1-amino-2-propanol) mixed inks (PPC-Cu/CuF-IPA) and sintered conductive copper films

Copper formate tetrahydrate (CuF, $Cu(HCOO)_2 \cdot 4H_2O$, Wako) and 1-amino-2-propanol (IPA, Junsei) with equal moles were mixed with a conditioning mixer for 40 min to prepare CuF-IPA complexes. Then the prepared PPC-capped copper fine particles were put into the CuF-IPA complex with mixing for another 16 min. Table 4.1 presents the compositions of the inks in detail. The total mole of IPA, CuF, and Cu atoms in the PPC-Cu particles was 16 mmol for all the inks. The moles of CuF and IPA in the prepared copper inks were the same. Inks with various molar ratios were prepared (Cu mol of PPC-Cu/Cu mol of CuF-IPA = 6/1, 2/1, and 2/3). The inks were named by the molar ratios. Then printed copper films were prepared by printing the inks on the Al_2O_3 substrate with a film thickness of 40 μm with a doctor blade. Finally, conductive copper films were obtained by sintering the printed films under a N_2 gas flow at 100 ℃ for various sintering time.

Table 4.1. The names of sample and compositions of the inks

Sample name	Composition		
	Cu atoms in PPC-Cu (mmol)	CuF (mmol)	IPA (mmol)
PPC-Cu/CuF-IPA 6/1	12	2	2
PPC-Cu/CuF-IPA 2/1	8	4	4
PPC-Cu/CuF-IPA 2/3	4	6	6

4.2.3 Preparation of PPC-Cu inks and films

Using conditioning mixer, prepared PPC-Cu particles (0.3 g, 4.7 mmol) were mixed with α-terpineol (0.3 g, 1.9 mmol, 95%, Kanto, Japan) for 18 min to prepare the inks. Then the inks were printed on the Al_2O_3 substrates with following sintering process for 1 h under a N_2 atmosphere at 100 ℃ and 150 ℃.

4.2.4 Characterization

The Scanning electron microscopy (SEM) images of the PPC-Cu particles and copper films were observed by a JEOL JSM-6701F field-emission-type SEM. X-ray diffraction (XRD) patterns were got by a Rigaku Miniflex-II diffractometer. A Shimadzu DTG-60H was used for thermogravimetric differential thermal analysis (TGA-DTA). The thermal desorption mass spectrometry measurements (TDMS, Ulvac, BGM-102) with thermogravimetry and differential thermal analyses (TG-DTA, Bruker, 2000SA) were used for study the decomposition of CuF-IPA complex and CuF. A four-point probe using a Mitsubishi Chemical Analytech Loresta-GP with an

ASP probe was to measure the resistivity of the conductive copper films. UV-Vis spectra were got by a Shimadzu UV-1800. Ethanol was used to dissolve the CuF-IPA complex (1 wt% of CuF-IPA complex in ethanol) to obtain the samples of UV-Vis measurement. A Fourier transform infrared spectrometer (FTIR, Jasco FT/IR-4600) was utilized for getting the FTIR spectra.

4.3 Results and discussion

4.3.1 Preparation and characterization of PPC-Cu particles

The PPC-Cu particles were prepared at 60 ℃ without any inert or reductive atmosphere. The characterization of PPC-Cu is presented in Fig. 4.1. The prepared PPC-Cu particles have a wide size distribution (154 ± 54 nm) according to Fig. 4.1b. This wide size distribution of the PPC-Cu particles could enhance contact between particles by forming a dense film, thus leading to low temperature sintering. After the sintering process, there are less remaining vacancy in the obtained conductive copper films due to the contacts between the large particles and small particles; this leads to low resistivity.[5] From the TG result in Fig. 4.1c, it is revealed that there was 2.2 wt% of PPC in the prepared PPC-Cu particles. The XRD pattern (Fig. 4.1d) indicates that all the detected peaks are corresponding to metallic copper without any copper oxide (Cu_2O, CuO, or other metastable phases[6,7]). This is because the well coating of PPC for copper particles.

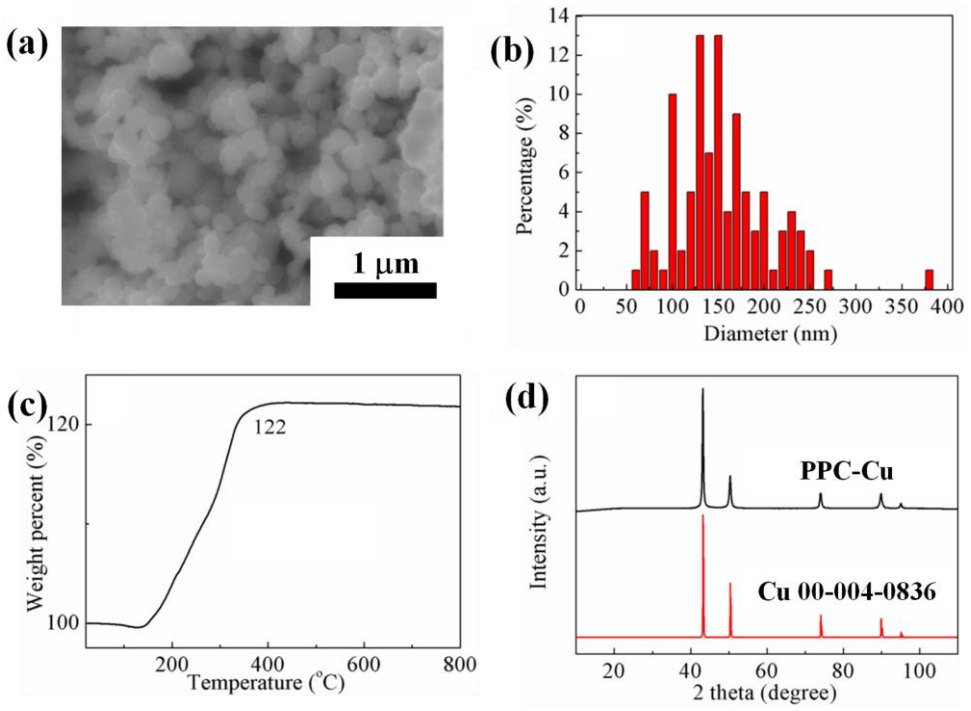

Fig. 4.1 (a) SEM image, (b) particle size distribution, (c) TG in air, and (d) XRD of the synthesized PPC-Cu particles.

4.3.2 Decomposition process of CuF-IPA complex

Fig. 4.2 shows the image of fabricated CuF-IPA complex which is a blue liquid and has a relatively high viscosity. It is well acknowledged that the interactions between IPA and Cu can lead to formation of stable five-membered metallacycle structures because of the hard soft acid base theory.[8] An UV-Vis spectroscopy measurement was taken to study the producing process of the CuF-IPA complexes (Fig. 4.3). From the UV results (Fig. 4.3), it is indicated that there was no obvious red/blue shift of the extinction peaks, proving that the ligand-field intensity did not change so much when varying the mixing time from 24 min to 56 min.[9] In this study, 40 min was chosen to obtain the CuF-IPA complex.

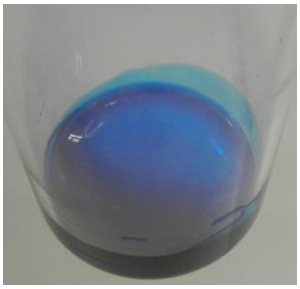

Fig. 4.2 Photo of CuF-IPA complex.

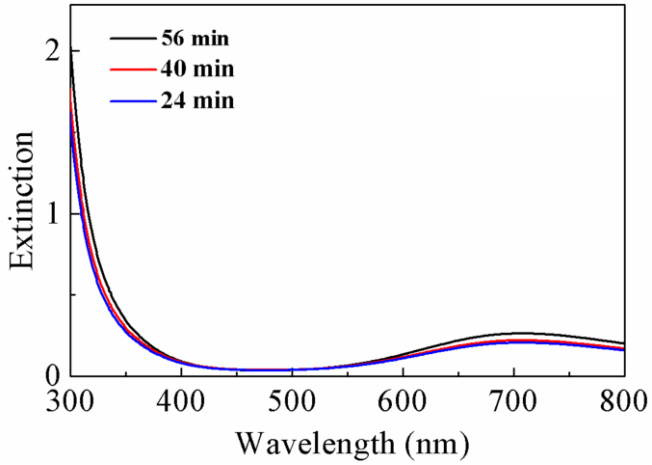

Fig. 4.3 UV-vis extinction spectra of the CuF-IPA complex prepared with various mixing periods.

Eqs. 1-3 shows the decomposition of CuF which can produce copper and other volatile products like H_2 and CO_2.

$$Cu(HCOO)_2 \rightarrow Cu(HCOO) + \tfrac{1}{2} H_2(g) + CO_2(g) \quad \text{(Eq. 1)}$$

$$Cu(HCOO) \rightarrow Cu(s) + \tfrac{1}{2} H_2(g) + CO_2(g) \quad \text{(Eq. 2)}$$

In total:

$$Cu(HCOO)_2 \rightarrow Cu(s) + H_2(g) + 2CO_2(g) \quad \text{(Eq. 3)}$$

IPA was found it can act as a reductant due to the secondary OH group in IPA and have the ability of reducing copper oxide to metallic copper under a N_2 gas flow.[10]

Figs. 4.4, 4.5 and 4.6 are the TGA and DTA/TGA-MS results to study the

decomposition of CuF as well as CuF-IPA complex. It is revealed that the decomposition of the CuF-IPA complex can take place at lower temperature compared with CuF, indicating that IPA can facilitate the decomposition of CuF due to its role as a reductant. The temperature for complete decomposition of the CuF-IPA was much lower than (~95 ℃) that of the CuF (Fig. 4.4). For the decomposition of CuF, it occurred from 183 ℃ to 236 ℃ by releasing of plenty of CO_2 and bound water, which can be demonstrated by the weight loss in Fig. 4.4 and the endothermic peak shown in Fig. 4.6. But for the decomposition of the CuF-IPA complex, it was more complicated.

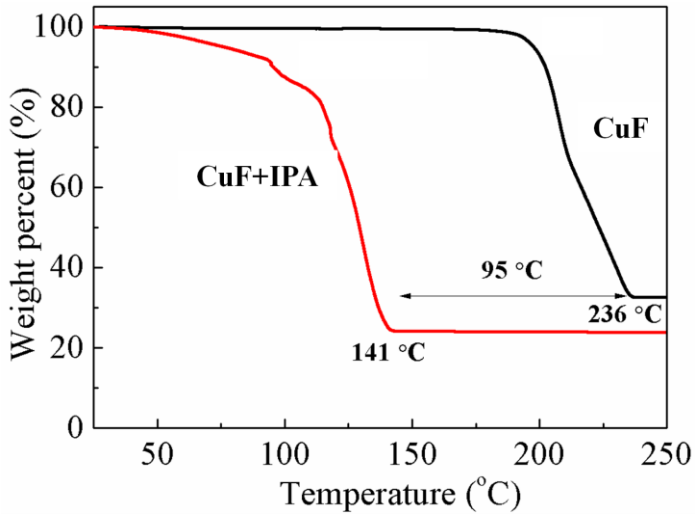

Fig. 4.4 TGA plots of CuF and CuF-IPA complexes (CuF:IPA=1:1, mol/mol) under a He gas flow.

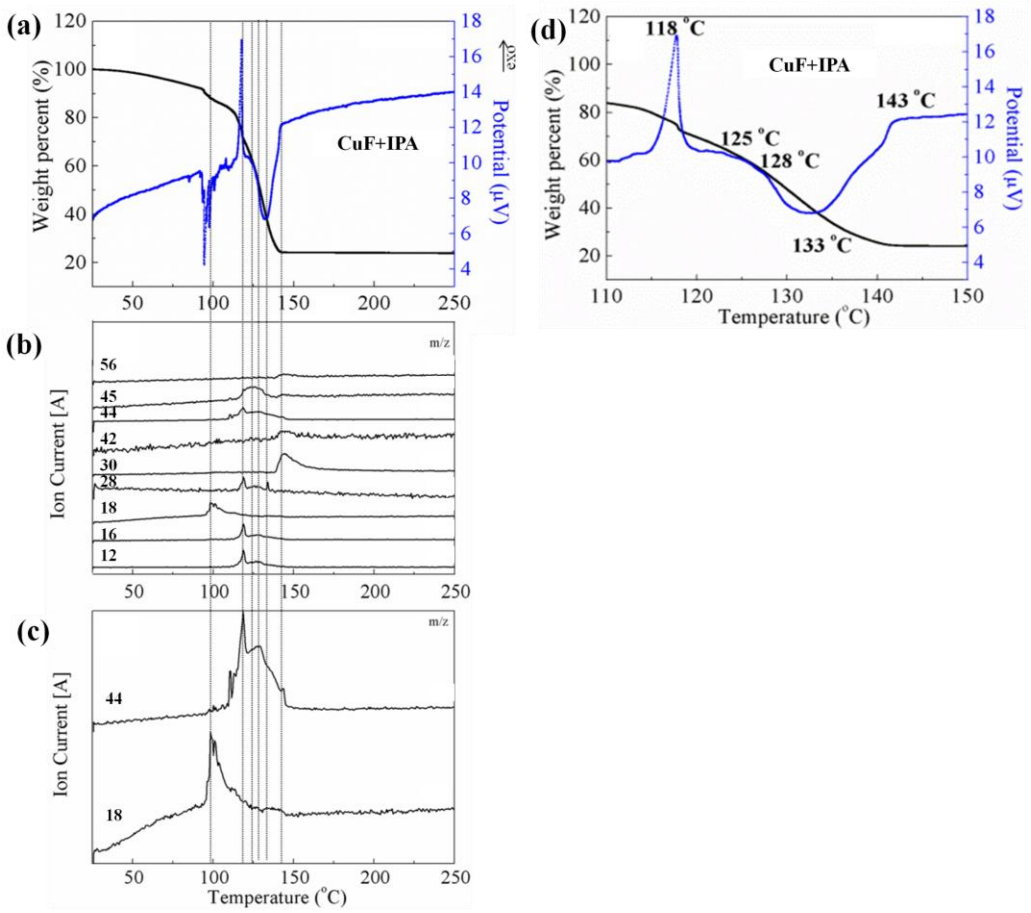

Fig. 4.5 DTA/TGA-MS of CuF-IPA complex (CuF:IPA=1:1, mol/mol) under a He gas flow: (a) DTA/TGA, (b) fragments obtained during the decomposition and corresponding MS results (mass to charge ratio (m/z) *versus* temperature), (c) magnification of MS spectra presented in (b) for m/z of 18 and 44, (d) DTA/TGA of CuF-IPA complex from 110 to 150 ℃. The mass to charge ratios (m/z), obtained as the main decomposition products and their fragments, were C (amu=12), CH_4 (amu=16), H_2O (amu=18), (CO or CH_2CH_2) (amu=28), (CH_4N) (amu=30), (CH_3CHCH_2) (amu=42), CO_2 (amu=44), HCOO (amu=45), and ($(CH_2)_2CO$) (amu=56).

Fig. 4.5 presents the DTA/TGA-MS data of the CuF-IPA complex. The main gaseous products generated during this process are shown in Figs. 4.5b and 4.5c. The evaporation of non-bound water and generation of a small quality of CO_2 happened at

~100 ℃ as shown Fig. 4.5c, demonstrating the decomposition of the CuF, to the lower valence states of copper, commenced (Eqs. 1–3). A large amount of Cu (II) was reduced to lower valence state of Cu (I) (Eq. 1), during which the formate, CO_2, C, and fragments from IPA (exothermic peaks at 118 ℃) were released. There are two exothermic DTA peaks (125 and 128 ℃ in Fig. 4.5d). During this process, Cu (I) was reduced to Cu (0) and CO_2 was produced by the release of second formate as shown in Eq. 2. In addition, the evaporation of formate, C, and fragments of IPA, happened. The endothermic peak at 133 ℃ was due to the evaporation of CO_2, bound water, and fragments of IPA.

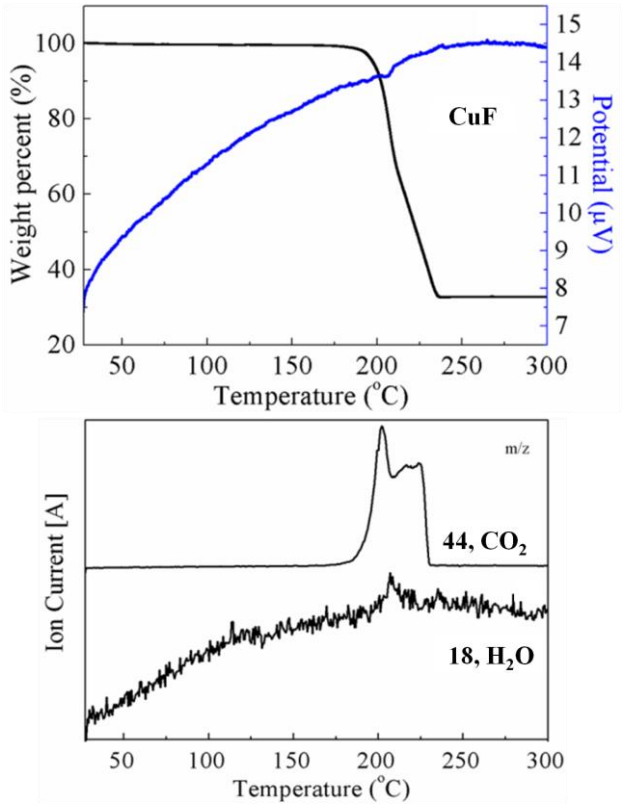

Fig. 4.6 DTA/TGA-MS of CuF. The mass to charge ratio (m/z) detected as decompostion product were CO_2 (amu=44) and H_2O (amu=18).

In total, the above demonstrated that the decomposition of the CuF-IPA complex, happened from ~100 ℃ and finished ~143 ℃.

4.3.3 Merits of PPC-capped copper particles and formation of copper film with PPC-Cu/CuF-IPA inks

Our group has demonstrated that the uniformity and packing density of the sintered copper films can be enhanced by using the mixing of copper complex and added commercially copper fine particles (~0.8 μm) as the inks. The conductive copper films with low resistivity were produced at 100 ℃.[4] This was due to the less vacancy of sintered copper films by the deposition of copper from CuF to fill in the space between the added copper particles. Smaller copper particles which also have a wide size distribution are favorable to further decreasing the resistivity of the obtained copper films sintered at low sintering temperature. But organic capping layers are generally essential for controlling the particles size and preventing particle oxidation.[11] These organic capping layers can inhibit the contacts among particles, causing high resistivity. The sintering at a higher temperature is usually needed to remove these organic layers.[12,13]

In this study, to use copper particles with a smaller size and wide size distribution and to prevent the high temperature sintering for the removal of the organic capping layers, a decomposable polymer, PPC, was chosen as a ligand for the preparation of copper particles. PPC as a kind of biodegradable and biocompatible polymer is an alternating copolymer of propylene oxide (PO) and carbon dioxide (~43% of total weight). Due to the use of carbon dioxide, the white pollution in the environment can

be reduced.[14-16] According to the TG of PPC (Fig. 4.7), it can be decomposed in the range from 200 ℃ to 250 ℃. However, the decomposition temperature becomes lower by an aminolysis reaction with amine or amino alcohol The aminolysis reaction is shown in Fig. 4.8.[17] Owing to the aminolysis of PPC, PPC cannot have effective steric stabilizations of the copper particles, leading to the coalescence of the copper particles.

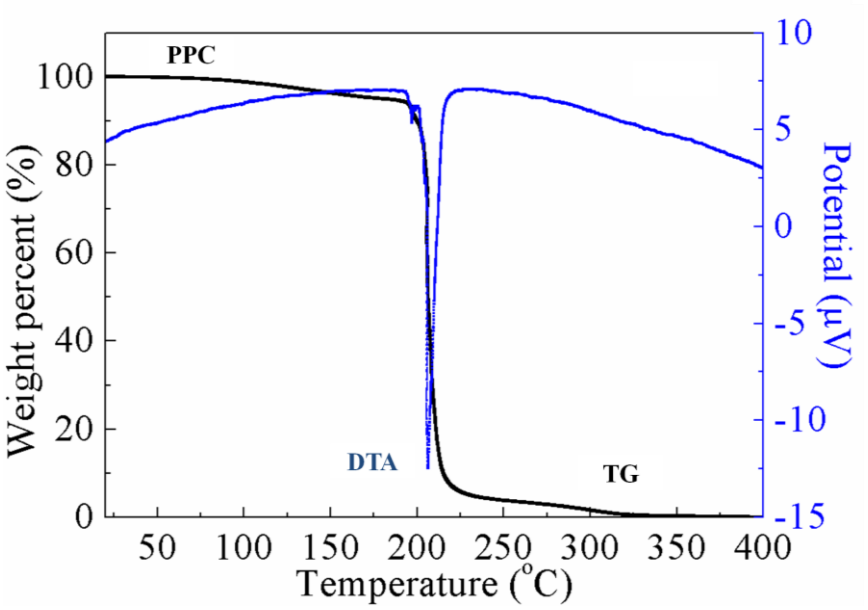

Fig. 4.7 DTA/TGA of PPC under a He gas flow.

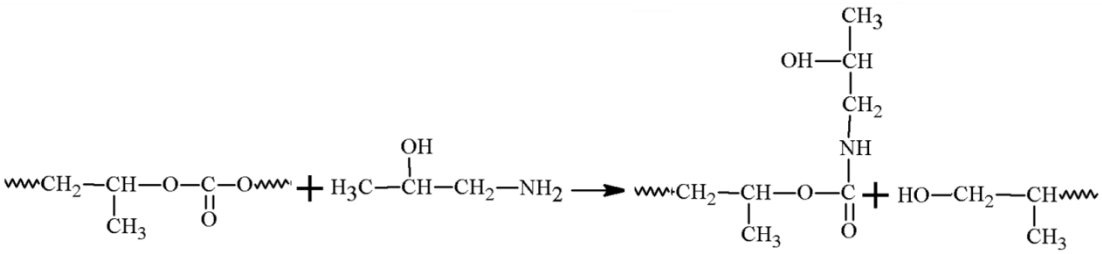

Fig. 4.8 The aminolysis reaction of PPC with IPA.

In this study, the influence of the PPC-Cu particles on the resistivity of obtained

copper films was studied. The resistivities of the conductive copper films obtained after sintering at 100 ℃ under a N_2 gas flow for 1 h were presented in Fig. 4.9; PPC-Cu/CuF-IPA mixed inks with various mole ratios as shown in Table 4.1 were used. The obtained copper films could achieved the resistivities of 1.5×10^{-6}, 8.8×10^{-7}, and 2.4×10^{-6} Ω m by using the PPC-Cu/CuF-IPA (6/1), PPC-Cu/CuF-IPA (2/1), PPC-Cu/CuF-IPA (2/3) inks, respectively. The resistivities of the conductive copper films obtained using the lowest (PPC-Cu/CuF-IPA 2/3 ink) and highest (PPC-Cu/CuF-IPA 6/1 ink) amounts of PPC-Cu particles, were 1–2 times higher than that of the conductive copper film obtained using the PPC-Cu/CuF-IPA 2/1 ink. The crystal structure and surface morphology of the sintered copper films were investigated to understand the underlying reason for the above results.

Fig. 4.10 exhibits XRD patterns of copper films obtained using various inks after sintering under a N_2 atmosphere for 1 h. There were only the peaks of metallic copper besides the peaks of Al_2O_3 substrate. No copper oxides were found. This can be ascribed to the released hydrogen gas produced during the decomposition of CuF, which help maintaining a reducing atmosphere. Moreover, IPA molecules released by the decomposition of CuF-IPA are beneficial to keeping a reducing environment.

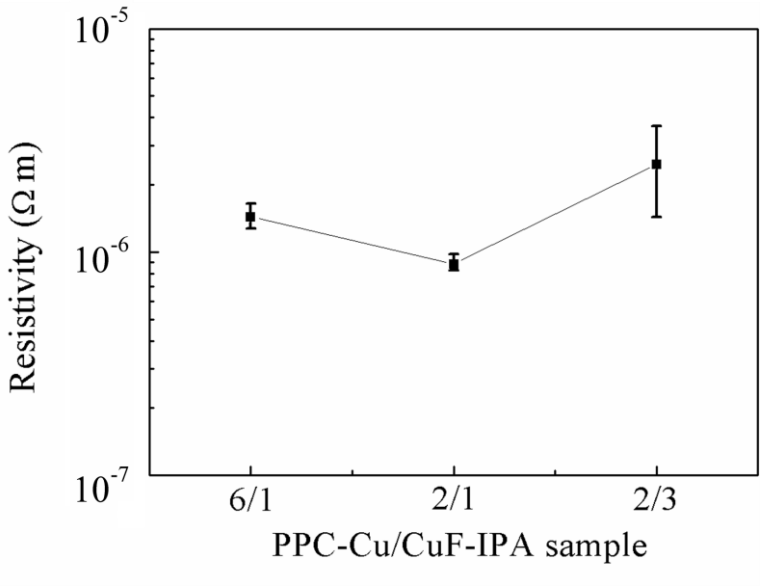

Fig. 4.9 Resistivities of the conductive copper films obtained using various copper inks shown in Table 4.1, after sintering process under a N_2 atmosphere at 100 ℃ for 1 h.

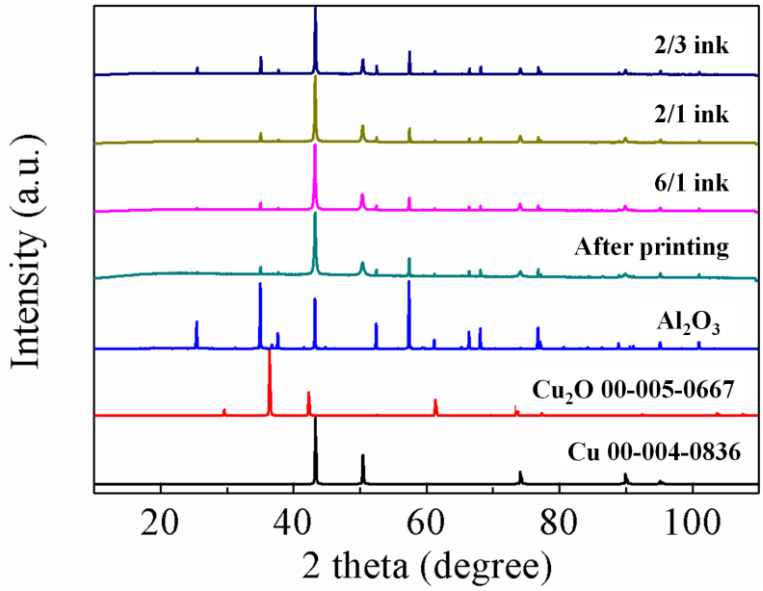

Fig. 4.10 XRD results of conductive copper films obtained following sintering process for 1 h at 100 ℃ by using PPC-Cu/CuF-IPA 6/1, 2/1 and 2/3 inks.

The surface morphologies and corresponding size distributions of the conductive copper films produced after sintering for 1 h were shown in Fig. 4.11. In all obtained conductive copper films, the copper particles have larger size than the added PPC-Cu

particles which were 154 ± 54 nm. These large copper particles were formed as a consequent of the coalescence products of copper produced by the decomposition of the CuF and the original PPC-Cu particles. The particle size in the copper films after sintering process became larger with fewer added PPC-Cu particles and more CuF-IPA complex in the prepared inks. Furthermore, for the copper films after sintering which used the ink containing the lowest amount of PPC-Cu particles (PPC-Cu/CuF-IPA 2/3 ink), the resistivity decreased rapidly with the sintering time increasing from 1 to 2 h. In contrast, there is negligible difference for the copper films after sintering which had more added PPC-Cu particles, as shown in Table 4.2 (PPC-Cu/CuF-IPA 2/1 and PPC-Cu/CuF-IPA 6/1 inks). In the case of the copper film after sintering which used PPC-Cu/CuF-IPA 2/3 ink, more contacts and less vacancy were observed after 2 h (Fig. 4.12) compared with those in the copper film after sintering for 1 h (Fig. 4.11c) (more contacts with less vacancy between particles can enhance the number of percolation paths, consequently leading to lower resistivity of film). According to the Gibbs-Thomson equation, the particles with the size more than 50 nm cannot melt at the sintering temperature of 100 ℃ (Fig. 4.11c). The possible reason for the resistivity decreasing dramatically from 1 h sintering to 2 h sintering, was that the complete decomposition of CuF after 2 h which can deposit copper on the surface of added PPC-Cu particles to form larger particles and in the space between added PPC-Cu particles, or the movement of generated nanoparticles which have higher chemical potential in the films after 1 h sintering to fill in the remaining space. Noticeable, the copper films obtained using the PPC-Cu/CuF-IPA 6/1 ink

which contains the largest amount of PPC-Cu particles also presented high resistivities as shown in Fig. 4.9 and Table 4.2. This can be explained by lots of PPC stabilizers. Excess PPC which could not be completely decomposed with the assist of IPA in the ink impeded the contacts among the copper particles, increasing the resistivity of the copper films. Based on the above results, it can be concluded that the PPC-Cu/CuF-IPA 2/1 ink (Fig. 4.13) was the optimal ink for producing conductive copper films with 8.8 × 10^{-7} Ω m of low resistivity at 100 ℃ of low sintering temperature within 1 h of short sintering time.

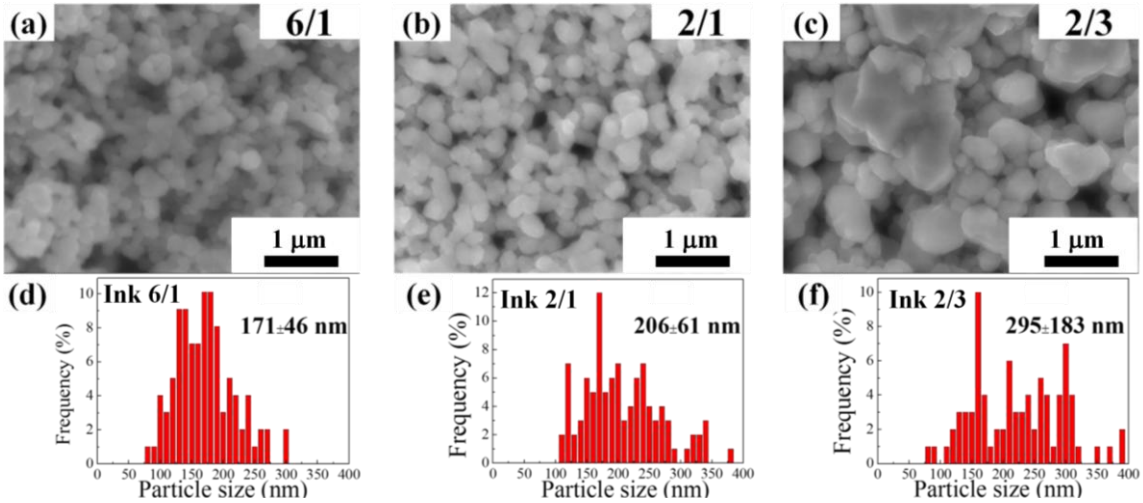

Fig. 4.11 Surface morphologies (a, b, and c) and relevant size distributions (d, e, and f) of the obtained copper films following sintering process at 100 ℃ for 1 h, by using PPC-Cu/CuF-IPA 6/1, 2/1 and 2/3 mixed inks, respectively.

Table 4.2. The resistivities of obtained copper films after sintering under a N_2 gas for various sintering time

Sample name	Sintering time (h) at 100 ℃	Resistivity ($\times 10^{-7}$ Ω m)
PPC-Cu/CuF-IPA 6/1	1	15.0
	2	18.0
PPC-Cu/CuF-IPA 2/1	1	8.8
	2	10.0
PPC-Cu/CuF-IPA 2/3	1	24.0
	2	10.0

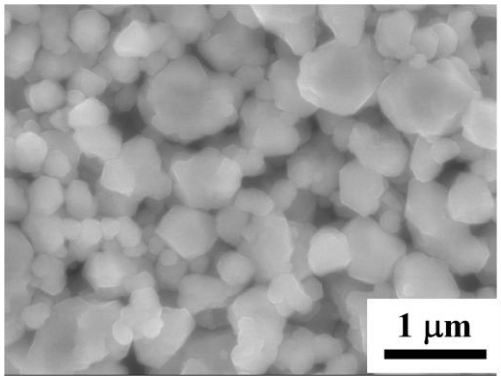

Fig. 4.12 Morphological image of copper films obtained following sintering process at 100 ℃ for 2 h, by using the PPC-Cu/CuF-IPA 2/3 ink.

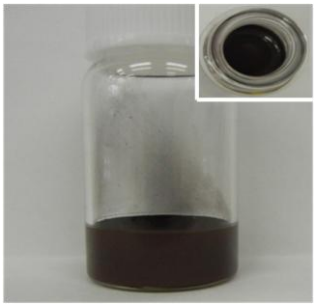

Fig. 4.13 Photo of PPC-Cu/CuF-IPA 2/1 ink.

The optimal sintering time was also studied using the PPC-Cu/CuF-IPA 2/1 ink. If the sintering time were 15 and 30 min, the resistivities of the obtained copper films were both over the measurement range. The SEM images f produced copper films which were sintered for 30 min and 1 h (Figs. 4.14a and 4.14b) exhibit plenty of organics and no contacts among particles. The decomposition of CuF did not completely finish, and such short sintering time was not enough for the aminolysis of PPC with IPA. When the sintering time was extended to 1 and 2 h, highly packed copper films were produced, as shown in Figs. 4.14c and 4.14d. The resistivities of copper films after sintering for 1 and 2 h, were 8.8×10^{-7} and 10.0×10^{-7} Ω m, respectively. Due to the negligible change about the resistivity of copper films, 1 h was decided to be the optimal time for obtaining conductive copper film.

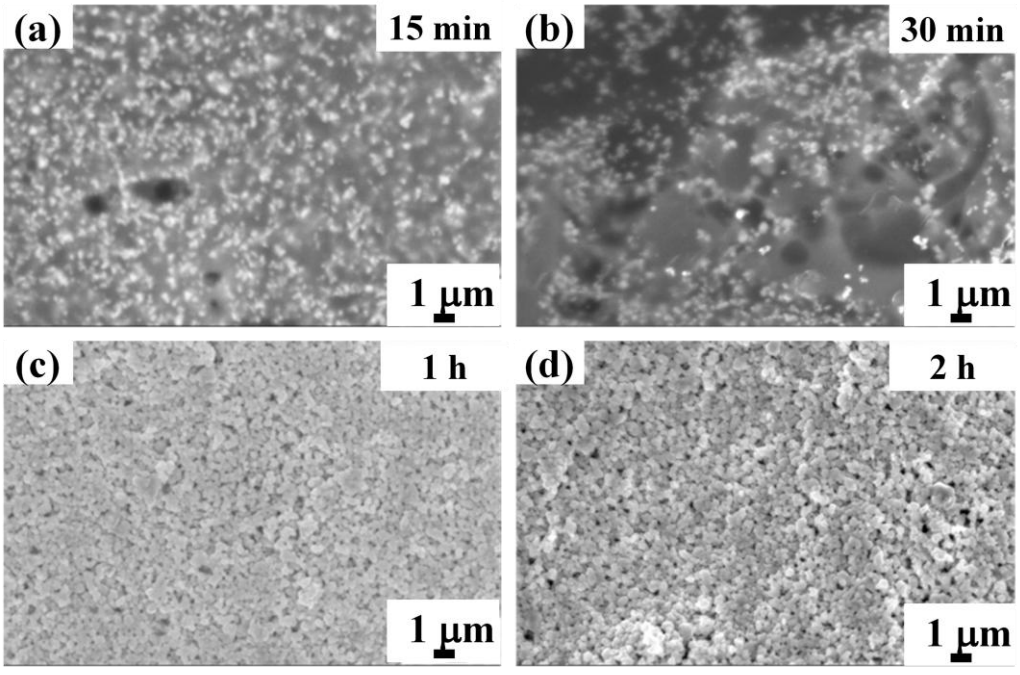

Fig. 4.14 Surface images of the copper films obtained using the PPC-Cu/CuF-IPA 2/1 ink after sintering process at 100 ℃ for (a) 15 min, (b) 30 min, (c) 1 h, and (d) 2 h.

4.3.4 Aminolysis of PPC with the assist of IPA at 100 ℃

Based on the above results and analyses, the decomposition of the PPC plays a critical role in producing conductive copper films with low resistivities. During the sintering process, PPC can be broken down into other molecules owing to the aminolysis with the assist of IPA as shown in Fig. 4.8, which causing the loss of effective protection for copper particles and low resistivity of obtained copper films. To demonstrate the aminolysis took place at 100 ℃ during the sintering process, FT-IR measurement was taken (Fig. 4.15). The amide group arising from the aminolysis reaction between carboxyl group in PPC and amino group in IPA can be detected. About the IR spectrum of PPC after heating at 100 ℃ under a N_2 gas flow, it was the same as that of the PPC without any heating. The IR spectrum of the mixture of PPC and IPA without heating process was the sum of the IPA and PPC spectra. In comparison, there are three obvious absorbance peaks representing the amide group in the mixture of the PPC and IPA after heating process at 100 ℃ for 3 h. These three absorbance peaks were 1560–1530 cm^{-1} (coupling of C-N stretching and N-H bending of amide II band), 1680–1640 cm^{-1} (C=O stretching of amide II band) and 3300–3250 cm^{-1} (N-H stretching of secondary amide).[18] In addition, about the peaks in the range of 3300–3250 cm^{-1}, they also included the peaks from O-H group in hydrolysis products or IPA. This IR result confirmed that the aminolysis of the PPC with IPA happened at 100 ℃ during the sintering process.

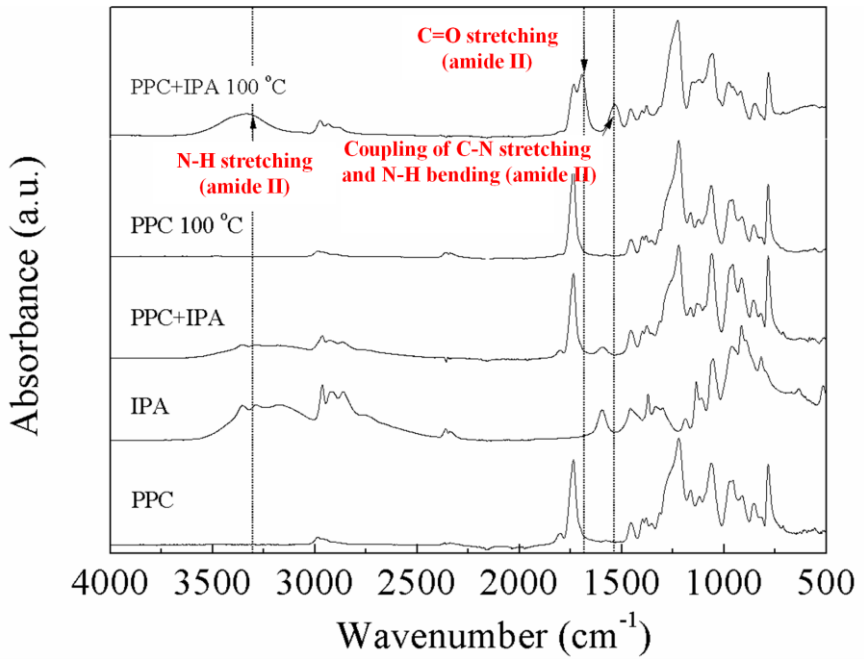

Fig. 4.15 FTIR spectra of PPC, IPA, and PPC+IPA (PPC:IPA=1:1, weight ratio) without heating, and PPC and PPC+IPA (PPC:IPA=1:1, weight ratio) after heating under a N_2 gas at 100 ℃ for 3 h.

In order to further confirm the significance of the mixture of PPC-Cu particle and CuF-IPA complex for achieving low resistivity of copper film, only the PPC-Cu particles were sintered under a N_2 flow. Fig. 4.16 shows the XRD patterns of the PPC-Cu particles after sintering at 100 ℃ and 150 ℃ under a N_2 flow for 1 h. The peaks corresponding to metallic copper without copper oxides were found. It should be noted that the resistivities of the copper films obtained using only PPC-Cu particles after sintering at 100 and 150 ℃ were both over range, as listed in Table 4.3. After sintering process at 100 ℃, the resistivity of the copper film obtained using only PPC-Cu particles was much higher than those of the copper films obtained by using the PPC-Cu/CuF-IPA inks (Table 4.2). This result can be explained with morphological images of sintered copper films. In comparison with the SEM images

of the sintered copper films using the PPC-Cu/CuF-IPA inks as shown in Fig. 4.11, the SEM images of the sintered copper film which used only PPC-Cu particles (Fig. 4.17) present much less contacts.

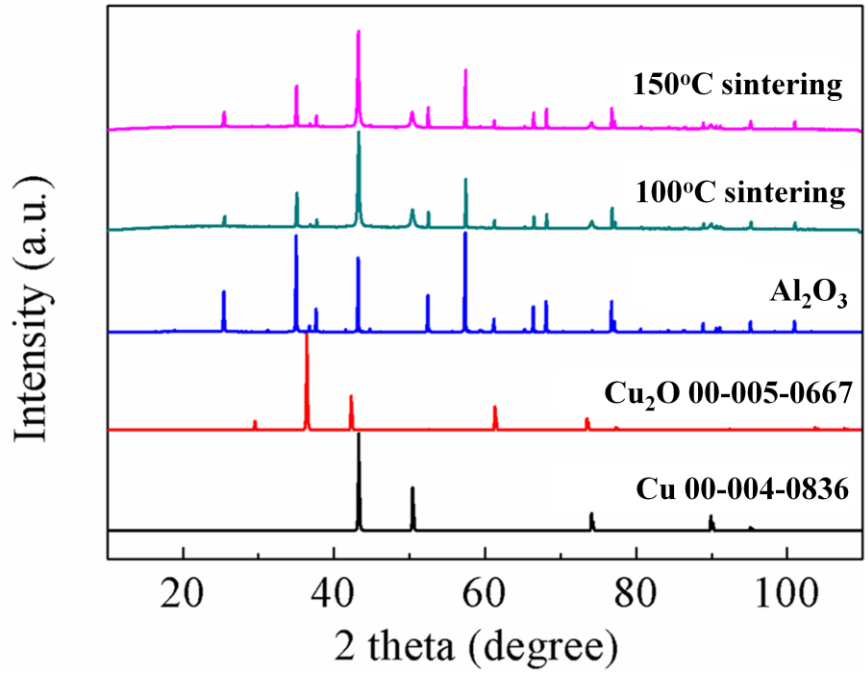

Fig. 4.16 XRD of the conductive copper films obtained using only PPC-Cu particles after sintering at 100 ℃ and 150 ℃ under a N_2 flow for 1 h.

Table 4.3. Resistivities of the conductive copper films obtained using only PPC-Cu particles after sintering under a N_2 flow for 1 h

Sintering temperature of particles (℃)	Resistivity (Ω m)
100	Over range
150	Over range

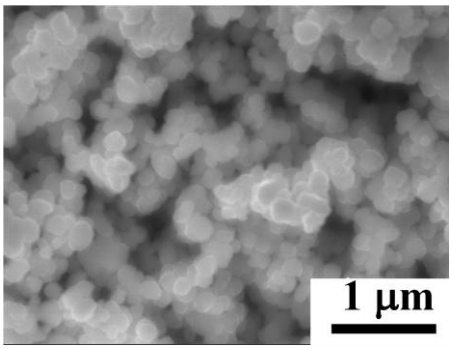

Fig. 4.17 Morphological image of PPC-Cu particles after sintering process under a N_2 gas at 100 ℃ for 1 h.

4.4 Conclusions

In this work, a new approach for achieving effective sintering of copper films at 100 ℃ were put forward by using PPC-Cu/CuF-IPA inks which contained decomposable polymer (PPC)-capped copper particles (154 ± 54 nm). It was demonstrated that the conductivity of sintered copper films were effectively enhanced by the aminolysis of the PPC with IPA. The contacts between PPC-Cu particles and the copper particles which were got from the decomposition of CuF and could deposit on the surfaces or spaces of PPC-Cu were improved by using PPC-Cu particles with small sizes and a wide size distribution, thus resulting in the producing of copper films with lower resistivity. Owing to the above dual promotional influences, a conductive copper film with low resistivity ($8.8 \times 10^{-7}\ \Omega$ m) after sintering process at 100 ℃ was obtained.

4.5 References

1 Magdassi, S.; Grouchko, M.; Berezin, O.; Kamyshny, A. Triggering the Sintering of Silver Nanoparticles at RoomTemperature. *ACS Nano* **2010**, *4*, 1943-1948.

2 Long, Y.; Wu, J.; Wang, H.; Zhang, X.; Zhao, N.; Xu, J. Rapid Sintering of Silver Nanoparticles in an Electrolyte Solution at Room Temperature and Its Application to Fabricate Conductive Silver Films Using Polydopamine as Adhesive Layers. *J. Mater. Chem.* **2011**, *21*, 4875-4881.

3 Grouchko, M.; Kamyshny, A.; Mihailescu, C. F.; Anghel, D. F.; Magdassi, S. Conductive Inks with a "Built-In" Mechanism That Enables Sintering at Room Temperature. *ACS Nano* **2011**, *5*, 3354-3359.

4 Yonezawa, T.; Tsukamoto, H.; Yong, Y.; Nguyen, M. T.; Matsubara, M. Low Temperature Sintering Process of Copper Fine Particles under Nitrogen Gas Flow with Cu 2^{+}-Alkanolamine Metallacycle Compounds for Electrically Conductive Layer Formation. *RSC Adv.* **2016**, *6*, 12048-12052.

5 Jeong, S.; Lee, S. H.; Jo, Y.; Lee, S. S.; Seo, Y.-H.; Ahn, B. W.; Kim, G.; Jang, G.-E.; Park, J.-U.; Ryu, B.-H. Air-Stable, Surface-Oxide Free Cu Nanoparticles for Highly Conductive Cu Ink and Their Application to Printed Graphene Transistors. *J. Mater. Chem. C* **2013**, *1*, 2704-2710.

6 Guan, R.; Hashimoto, H.; Kuo, K. H. Electron-Microscopic Study of the Structure of Metastable Oxides Formed in the Initial Stage of Copper Oxidation. II. Cu_8O. *Acta Crystallogr., Sect. B: Struct. Sci.* **1984**, *40*, 560-566.

7 Guan, R.; Hashimoto, H.; Kuo, K. H. Electron-Microscopic Study of the Structure of Metastable Oxides Formed in the Initial Stage of Copper Oxidation. III. $Cu_{64}O$. *Acta Crystallogr., Sect. B: Struct. Sci.* **1985**, *41*, 219-225.

8 Farraj, Y.; Grouchko, M.; Magdassi, S. Self-Reduction of a Copper Complex MOD Ink for Inkjet Printing Conductive Patterns on Plastics. *Chem. Commun.* **2015**, *51*, 1587-1590.

9 Faust, B. *Modern Chemical Techniques: An Essential Reference for Students and Teachers*; Royal Society of Chemistry, 1997.

10 Hokita, Y.; Kanzaki, M.; Sugiyama, T.; Arakawa, R.; Kawasaki, H. High-Concentration Synthesis of Sub-10-nm Copper Nanoparticles for Application to Conductive Nanoinks. *ACS Appl. Mater. Interfaces* **2015**, *7*, 19382-19389.

11 Yonezawa, T.; Uchida, Y.; Tsukamoto, H. X-Ray Diffraction and High-Resolution TEM Observations of Biopolymer Nanoskin-Covered Metallic Copper Fine Particles: Preparative Conditions and Surface Oxidation States. *Phys. Chem. Chem. Phys.* **2015**, *17*, 32511-32516.

12 Yong, Y.; Yonezawa, T.; Matsubara, M.; Tsukamoto, H. The Mechanism of

Alkylamine-Stabilized Copper Fine Particles Towards Improving the Electrical Conductivity of Copper Films at Low Sintering Temperature. *J. Mater. Chem. C* **2015**, *3*, 5890-5895.

13 Zhang, Y.; Zhu, P.; Li, G.; Zhao, T.; Fu, X.; Sun, R.; Zhou, F.; Wong, C. Facile Preparation of Monodisperse, Impurity-Free, and Antioxidation Copper Nanoparticles on a Large Scale for Application in Conductive Ink. *ACS Appl. Mater. Interfaces* **2014**, *6*, 560-567.

14 Li, X. H.; Meng, Y. Z.; Zhu, Q.; Tjong, S. C. Thermal Decomposition Characteristics of Poly(propylene carbonate) Using TG/IR and Py-GC/MS Techniques. *Polym. Degrad. Stab.* **2003**, *81*, 157-165.

15 Lin, S.; Yu, W.; Wang, X.; Zhou, C. Study on the Thermal Degradation Kinetics of Biodegradable Poly (propylene carbonate) during Melt Processing by Population Balance Model and Rheology. *Ind. Eng. Chem. Res.* **2014**, *53*, 18411-18419.

16 Nakano, K.; Hashimoto, S.; Nakamura, M.; Kamada, T.; Nozaki, K. Stereocomplex of Poly(propylene carbonate): Synthesis of Stereogradient Poly(propylene carbonate) by Regio- and Enantioselective Copolymerization of Propylene Oxide with Carbon Dioxide. *Angew. Chem., Int. Ed.* **2011**, *50*, 4868-4871.

17 Zhong, X.; Lu, Z.; Valtchev, P.; Wei, H.; Zreiqat, H.; Dehghani, F. Surface Modification of Poly(Propylene Carbonate) by Aminolysis and Layer-by-Layer Assembly for Enhanced Cytocompatibility. *Colloids Surf., B* **2012**, *93*, 75-84.

18 Stuart, B. H. *Infrared Spectroscopy: Fundamentals and Applications*; John Sons, Ltd.: Chichester, U. K., 2004.

5. Concluding Remarks

In the first chapter, the introduction about the materials for printed electronics has been introduced. Copper inks were chosen as the research topic due to its low cost, low resistivity (1.7×10^{-8} Ω m, similar to that of silver) and high electromigration resistance. However, copper particles have the problems of oxidation and high sintering temperature. To realize low resistivities of the sintered conductive copper films at low sintering temperatures (≤ 200 ℃), new approaches were developed.

In the second chapter, instead of the common way (decreasing particle size to nanoscale) to reduce the sintering temperature, a new approach was put forward. A two-step process, during which an easy thermal oxidation procedure was introduced to enhance the contacts among particles, was investigated to achieve effective coalescence and sintering of copper fine particles (>100 nm). For the first step, copper fine particles with an average size of 280 nm were prepared using a facile one-pot reaction with D-isoascorbic acid as a mild reductant. For the second step, the synthesized copper fine particles were sintered by an oxidative preheating process and following reductive sintering under a 3% H_2 in N_2 gas. During the critical oxidative preheating process, the connections among particles were enhanced by generating convex surfaces, nanorods or nanoparticles. Consequently, the copper films after sintering 200 ℃ and 250 ℃ could have the resistivities of 12.2×10^{-8} and 7.8×10^{-8} Ω m, respectively.

In the third chapter, copper-based MOD inks with simplicity and scalability were

discussed for achieving low resistivity at a lower sintering temperature. The mixture of copper complex and added copper particles were used for preparation of ink. The choice of various copper sources (i.e., copper (II) acetate monohydrate and copper (II) formate tetrahydrate) in MOD inks was studied. Commercially copper fine particles with various sizes (0.4-2.5 μm) and prepared PVP-Cu particles were added into the inks to replace the organic components for lower resistivity and higher reliability of the conductive copper films. The effect of size of added copper particles and organic residuals on the resistivity of obtained copper films was also discussed. It was testified the general applicability of mixing copper complex with added copper particles as the ink for low resistivity of copper film at low sintering temperature. The copper film obtained using the ink containing 0.4 μm of added copper particles after sintering at 120 ℃ under a N_2 gas achieved 2.6×10^{-7} Ω m of low resistivity. By using the ink which contains PVP-Cu particles as added copper particles, a conductive copper film with low resistivity (7×10^{-6} Ω m) can also be obtained after sintering at 100 ℃ under a N_2 gas.

In the fourth chapter, to further reduce the resistivity, decomposable polymer (polypropylene carbonate, PPC) capped copper particles with a wide size distribution as a main part and a copper formate/1-amino-2-propanol (CuF-IPA) complex which is self-reducible as an additive were prepared for low temperature sintering. The surface modification of PPC with IPA, smaller particles with a wide size distribution, and self-reducible copper complex play important roles in obtaining conductive copper films with a low resistivity at a low sintering temperature. A low resistivity (8.8×10^{-7}

Ω m) after sintering at 100 ℃ without any reductive gases was achieved.

The aforementioned approaches and prepared inks developed in our work have great potential used for flexible printing electronic devices with low-cost.

List of Publications

[1] Yingqiong Yong, Tetsu Yonezawa, Masaki Matsubara, Hiroki Tsukamoto

Journal of Materials Chemistry C, 2015, 3, 5890-5895. (**Selected as front cover**)

The mechanism of alkylamine-stabilized copper fine particles towards improving electrical conductivity of copper films at low sintering temperature

[2] Tetsu Yonezawa, Hiroki Tsukamoto, Yingqiong Yong, Mai Thanh Nguyen, Masaki Matsubara

RSC Advances, 2016, 6, 12048-12052.

Low temperature sintering process of copper fine particles under nitrogen gas flow with Cu^{2+}-alkanolamine metallacycle compounds for electrically conductive layer formation

[3] Masaki Matsubara, Tetsu Yonezawa, Takato Minoshima, Hiroki Tsukamoto, Yingqiong Yong, Yohei Ishida, Mai Thanh Nguyen, Hiroki Tanaka, Kazuki Okamoto, Takuya Osaka

RSC Advances, 2015, 5, 102904-102910.

Proton-assisted low-temperature sintering of Cu fine particles stabilized by a proton-initiating degradable polymer

[4] Yingqiong Yong, Mai Thanh Nguyen, Tetsu Yonezawa, Masaki Matsubara, Hiroki Tsukamoto, Tengfei Zhang, Shigehito Isobe, and Yuki Nakagawa

Have been submitted and under review.

Use of decomposable polymer-coated submicron Cu particles with effective additive for production of highly conductive Cu films at low sintering temperature

[5] Yingqiong Yong, Mai Thanh Nguyen, Tetsu Yonezawa, Masaki Matsubara, Hiroki Tsukamoto.

Under review.

Systematic study of copper-based metal-organic decomposition inks using the mixture of copper complex and added copper particles for low temperature sintering

List of Presentations and Posters

1 Yingqiong Yong, Tetsu Yonezawa, Hiroki Tsukamoto. Oxidative Preheating Effects on Annealing Process of One-Pot Synthesized Copper Fine Particles Capped by Octylamine. The Summer Session of Hokkaido Branch of Japan Institute of Metals and Materials and the Iron and Steel Institute of Japan. Hokkaido University. 2014/07/28. Poster.

2 Yingqiong Yong, Masaki Matsubara, Hiroki Tsukamoto, Tetsu Yonezawa. Preparation of Copper Fine Particles and Study of Oxidative Preheating Process for Highly Conductive Copper Films at Low Temperatures. The 50th Hokkaido Branch Symposium of Japan Society of Applied Physics / 11th Hokkaido District Symposium of Japan Optical Society. Asahikawa City Worker's Welfare Center. 2015/01/10. Oral.

3 Yingqiong Yong, Masaki Matsubara, Hiroki Tsukamoto, Tetsu Yonezawa. One-Pot Synthesized Copper Fine Particles and Study of Oxidative Preheating Process for Improving the Conductivity of Copper Films. 2015 Winter Seminar of Hokkaido Branch of the Chemical Society of Japan. Hokkaido University. 2015/01/27. Oral.

4 Yingqiong Yong, Masaki Matsubara, Hiroki Tsukamoto, Tetsu Yonezawa. Study on Oxidative Preheating Process of Printed Copper Films for Enhanced Electrical Conductivity. 3rd International Doctoral Student Symposium on Material Science. Hokkaido University. 2015/02/26. Oral.

5 Yingqiong Yong, Masaki Matsubara, Hiroki Tsukamoto, Tetsu Yonezawa. Synthesis of Copper Fine Particles and Study of Oxidative Preheating Process for Obtaining Highly Conductive Copper Films. The 95th Annual Meeting of the Chemical Society of Japan. Nippon University. 2015/03/26. Oral

6 Yingqiong Yong, Masaki Matsubara, Hiroki Tsukamoto, Tetsu Yonezawa. A New Route to Highly Conductive Copper Films at Low Temperatures. The Summer Session of Hokkaido Branch of Japan Institute of Metals and Materials and the Iron and Steel Institute of Japan. Muroran Institute of Technology. 2015/07/17. Poster.

7 Yingqiong Yong, Masaki Matsubara, Hiroki Tsukamoto, Tetsu Yonezawa. Effect of Oxidative Preheating Process on Sintering of One-Pot Synthesized Copper Fine Particles Capped by Octylamine. 64th SPSJ Annual Meeting. Sapporo Convention Center. 2015/05/27. Oral.

8 Yingqiong Yong, Masaki Matsubara, Hiroki Tsukamoto, Tetsu Yonezawa. Low Temperature Sintering Mechanism of Octylamine-Stabilized Copper Fine Particles for Improving Conductivity of Copper Films. 2015 International Conference of Colloids and Interface Science. National Taiwan University of Science and Technology, Taipei, Taiwan. 2015/07/22. Oral.

Acknowledgement

This research was completed under the supports of many persons. I would like to express my deep gratitude to them.

This research was promoted under the guidance of Professor Dr. Tetsu Yonezawa. I really appreciate for the help of Yonezawa sensei. He gave me the chance to study in this laboratory. Many great suggestions and discussions were given. In this laboratory, much chemical knowledge was learnt. In addition, Yonezawa sensei gave me many chances, including conference chances and collaboration chances with other laboratories or universities, to broaden my horizon.

I thank Mr. Hiroki Tsukamoto sincerely. Tsukamoto san helped me a lot about my experiments. At the beginning of starting my research, he was always patient with training me to use experimental equipments. Furthermore, I got many suggestions and discussions from him.

I thank Dr. Masaki Matsubara very much. Even just several months under the guidance of him, I have learnt many things, especially about the chemistry. I really thank Matsubara san for his valuable suggestions and kind supports.

I am deeply grateful to Assistant Professor Dr. Mai Thanh Nguyen. Mai san helped

me a lot about my papers and thesis as well as the experiments. Essential discussions and sincere encouragement were obtained. I have learnt many things from her. I gratefully appreciate Mai san.

I would like to express my cordial thanks to Assistant Professor Dr. Ishida Yohei. Even though he is not the person who directly guided me, he gave me many usefully suggestions and encouragements. His active supports were indispensable for my research.

I also thank Associate Professor Dr. Sakairi Masatoshi sincerely for giving me many useful advices for my study as well as my life.

I would like to thank Specially Appointed Assistant Professor Dr. Yongming Wang for the help of using TEM; I thank Associate Professor Dr. Shigehito Isobe, Dr. Tengfei Zhang and Dr. Yuki Nakagawa for using TG-MS; I thank Associate Professor Dr. Tatsufumi Okino for using of ESI. I am grateful to their help for my experiments.

I appreciate all the members in the Laboratory of Novel Materials Hybrid Engineering, especially Mr. Sumi Taiki who has helped me a lot for my life in Japan.

I am indebted to Chinese government who supplied me the scholarship for studying and living in Japan and Hokkaido University for offer me such a great environment

for study and research.

I would like to express sincere gratitude to my parents. I thank them for supporting me mentally and teaching me many things to overcome difficulties.

Reproduced from Ref. 12 (Chapter 4) with permission from the Royal Society of Chemistry.

Yingqiong Yong